



Calhoun: The NPS Institutional Archive
DSpace Repository

Theses and Dissertations

1. Thesis and Dissertation Collection, all items

1994-03

Elimination of electromagnetic interference to receivers and sensitive equipment generated by switching systems

Stelioudakis, Emmanuel

Monterey, California. Naval Postgraduate School

<https://hdl.handle.net/10945/42953>

This publication is a work of the U.S. Government as defined in Title 17, United States Code, Section 101. Copyright protection is not available for this work in the United States.

Downloaded from NPS Archive: Calhoun



Calhoun is the Naval Postgraduate School's public access digital repository for research materials and institutional publications created by the NPS community. Calhoun is named for Professor of Mathematics Guy K. Calhoun, NPS's first appointed -- and published -- scholarly author.

Dudley Knox Library / Naval Postgraduate School
411 Dyer Road / 1 University Circle
Monterey, California USA 93943

<http://www.nps.edu/library>

AD-A281 643



①

NAVAL POSTGRADUATE SCHOOL
Monterey, California



THESIS

DTIC
ELECTE
JUL 19 1994
S G D

**ELIMINATION OF ELECTROMAGNETIC
INTERFERENCE TO RECEIVERS AND
SENSITIVE EQUIPMENT GENERATED BY
SWITCHING SYSTEMS**

by

Emmanuel Stelioudakis

March, 1994

Thesis Advisor:

Richard W. Adler

Approved for public release; distribution is unlimited.

DTIC QUALITY INSPECTED 5

94-22065



2898

94 7 14 019

REPORT DOCUMENTATION PAGE			Form Approved OMB No. 0704	
Public reporting burden for this collection of information is estimated to average 1 hour per response, including the time for reviewing instruction, searching existing data sources, gathering and maintaining the data needed, and completing and reviewing the collection of information. Send comments regarding this burden estimate or any other aspect of this collection of information, including suggestions for reducing this burden, to Washington Headquarters Services, Directorate for Information Operations and Reports, 1215 Jefferson Davis Highway, Suite 1204, Arlington, VA 22202-4302, and to the Office of Management and Budget, Paperwork Reduction Project (0704-0188) Washington DC 20503.				
1. AGENCY USE ONLY (Leave blank)	2. REPORT DATE March 14, 1994	3. REPORT TYPE AND DATES COVERED Master's Thesis		
4. TITLE AND SUBTITLE ELIMINATION OF ELECTROMAGNETIC INTERFERENCE TO RECEIVERS AND SENSITIVE EQUIPMENT GENERATED BY SWITCHING SYSTEMS		5. FUNDING NUMBERS		
6. AUTHOR(S) Stelioudakis, Emmanuel				
7. PERFORMING ORGANIZATION NAME(S) AND ADDRESS(ES) Naval Postgraduate School Monterey CA 93943-5121		8. PERFORMING ORGANIZATION REPORT NUMBER		
9. SPONSORING/MONITORING AGENCY NAME(S) AND ADDRESS(ES) Naval Postgraduate School Monterey, CA 93943-5121		10. SPONSORING/MONITORING AGENCY REPORT NUMBER		
11. SUPPLEMENTARY NOTES The views expressed in this thesis are those of the author and do not reflect the official policy or position of the Department of Defense or the U.S. Government.				
12a. DISTRIBUTION/AVAILABILITY STATEMENT Approved for public release; distribution is unlimited.		12b. DISTRIBUTION CODE A		
13. ABSTRACT (maximum 200 words) Recently installed equipment in naval receiving sites such as digital telephone switching systems, uninterruptible power supplies, laser printers etc., induce Electromagnetic Interference (EMI) into receiver systems, thus limiting the performance of the receiving site. EMI is injected into receiver systems by conducted, inductive and capacitive paths associated with poor compartment shielding, grounds, or cable shielding. In this thesis, the MITEL SX-20 automatic digital telephone switching system is studied as an EMI source. Temporal and spectral properties of EMI generated by the MITEL SX-20 system are examined over a frequency range of 0 to 100 MHz. The effectiveness of a Barrier, Filter and Ground architecture in containing/eliminating the generated EMI is tested under various operating conditions. Possible solutions are proposed for similar EMI sources.				
14. SUBJECT TERMS RADIO NOISE, MAN-MADE NOISE, EMI/RFI, ELECTROMAGNETIC INTERFERENCE, RADIO FREQUENCY INTERFERENCE			15. NUMBER OF PAGES 79	16. PRICE CODE
17. SECURITY CLASSIFICATION OF REPORT Unclassified	18. SECURITY CLASSIFICATION OF THIS PAGE Unclassified	19. SECURITY CLASSIFICATION OF ABSTRACT Unclassified	20. LIMITATION OF ABSTRACT	

Approved for public release; distribution is unlimited.

**ELIMINATION OF ELECTROMAGNETIC INTERFERENCE TO
RECEIVERS AND SENSITIVE EQUIPMENT GENERATED BY
SWITCHING SYSTEMS**

by

**Emmanuel Stelioudakis
Lieutenant JG, Hellenic Navy
B.S.E.E., Hellenic Naval Academy, 1986**

**Submitted in partial fulfillment
of the requirements for the degree of**

MASTER OF SCIENCE IN ELECTRICAL ENGINEERING

from the

NAVAL POSTGRADUATE SCHOOL

March 1994

Author:

[Redacted Signature]

Emmanuel Stelioudakis

Approved by:

[Redacted Signature]

Richard W. Adler, Thesis Advisor

[Redacted Signature]

Wilbur R. Vincent, Second Reader

[Redacted Signature]

**Michael A. Morgan, Chairman
Department of Electrical and Computer Engineering**

ABSTRACT

Recently installed equipment in naval receiving sites such as digital telephone switching systems, uninterruptible power supplies, laser printers etc., induce Electromagnetic Interference (EMI) into receiver systems, thus limiting the performance of the receiving site. EMI is injected into receiver systems by conducted, inductive and capacitive paths associated with poor compartment shielding, grounds, or cable shielding. In this thesis, the MITEL SX-20 automatic digital telephone switching system is studied as an EMI source. Temporal and spectral properties of EMI generated by the MITEL SX-20 system are examined over a frequency range of 0 to 100 MHz. The effectiveness of a Barrier, Filter and Ground architecture in containing/eliminating the generated EMI is tested under various operating conditions. Possible solutions are proposed for similar EMI sources.

Accession For	
NTIS	CRA&I <input checked="checked" type="checkbox"/>
DTIC	TAB <input type="checkbox"/>
Unannounced <input type="checkbox"/>	
Justification _____	
By _____	
Distribution /	
Availability Codes	
Dist	Avail and/or Special
A-1	

TABLE OF CONTENTS

I.	INTRODUCTION	1
A.	MOTIVATION FOR THIS THESIS	1
B.	OUTLINE OF THE PROBLEM	2
C.	OVERVIEW OF THE THESIS	2
II.	THEORETICAL BACKGROUND AND RELATED WORK ..	4
A.	EXTERNAL EMI SOURCES	4
B.	INTERNAL EMI SOURCES	5
III.	INTEGRATED BARRIER, FILTER AND GROUND PLAN ..	7
A.	TOPOLOGICAL APPROACH	7
B.	BARRIER	8
C.	FILTERS	11
D.	GROUNDING	12
IV.	EXPERIMENT IMPLEMENTATION	14

A.	GENERAL CONSIDERATIONS	14
1.	Time	14
2.	Ambient noise	14
B.	MITEL SX-20 DIGITAL TELEPHONE SWITCHING SYSTEM	15
1.	Chassis	17
2.	Printed Circuit Cards	17
3.	Primary Power Supply	18
4.	Cooling Fan	18
5.	MITEL SUPERSET-3 Telephone Set	18
C.	INSTRUMENTATION	20
1.	Description	20
2.	Unmodified MITEL SX-20 Set-up	22
3.	Modified MITEL SX-20 Set-up	24
V.	UNMODIFIED MITEL SX-20 MEASUREMENTS	27
A.	GENERAL APPROACH	27
B.	GROUND CABLE MEASUREMENTS	28
C.	TELEPHONE LINE MEASUREMENTS	33

D.	POWER LINE MEASUREMENTS	42
VI.	MODIFIED MITEL SX-20 MEASUREMENTS	46
A.	GENERAL CONSIDERATIONS	46
B.	GROUND CABLE MEASUREMENTS	46
C.	TELEPHONE LINE MEASUREMENTS	50
D.	POWER LINE MEASUREMENTS	53
VII.	CONCLUSIONS AND RECOMMENDATIONS	60
A.	CONCLUSIONS	60
B.	RECOMMENDATIONS	62
	LIST OF REFERENCES	63
	INITIAL DISTRIBUTION LIST	65

LIST OF FIGURES

Figure 1. Interference From a Fluorescent Lamp [Ref. 1]	4
Figure 2. Typical Internal EMI Sources [Ref. 9]	5
Figure 3. Barrier, Filter and Ground (BFG) Configuration for a UPS .	8
Figure 4. Attenuation of an Electromagnetic Wave by a Metallic Barrier [Ref. 1]	9
Figure 5. Typical Shielded Enclosure Discontinuities [Ref. 1]	10
Figure 6. Power-Line Filter Configurations [Ref.5]	11
Figure 7. Good and Bad Ground Penetrations [Ref. 5]	13
Figure 8. MITEL SX-20 Automatic Digital Telephone Switching System	16
Figure 9. MITEL SX-20 Block Diagram [Ref. 15]	19
Figure 10. 3-Axis Display [Ref. 4]	21
Figure 11. Unmodified MITEL SX-20 Set-Up	22
Figure 12. Data Processing Channel	23
Figure 13. Modified MITEL SX-20 Set-Up	24
Figure 14. Aluminum Cabinet for MITEL SX-20 System	25
Figure 15. EMI Current on MITEL SX-20 Ground Cable	29

Figure 16. Ground Cable Transient Response	31
Figure 17. EMI Current on MITEL SX-20 Ground Cable	32
Figure 18. EMI Current on MITEL SX-20 Telephone Line	34
Figure 19. EMI Current on Telephone Line during Turn-On	35
Figure 20. EMI Current on MITEL SX-20 Telephone Line	37
Figure 21. Slanting Lines of Noise on MITEL SX-20 Telephone Line	38
Figure 22. Telephone Line Transient Response	40
Figure 23. EMI Current on MITEL SX-20 Telephone Line	41
Figure 24. Power-Line Transient Response	43
Figure 25. EMI Current on MITEL SX-20 Power-Line	44
Figure 26. EMI Current on Ground Cable Inside the Cabinet	48
Figure 27. EMI Current on Ground Cable Outside the Cabinet	49
Figure 28. EMI Current on Telephone Line Inside the Cabinet	51
Figure 29. EMI Current on Telephone Line Outside the Cabinet	52
Figure 30. Ambient Noise on Telephone Line Outside/inside the Cabinet	54
Figure 31. EMI Current on Power-Line Inside the Cabinet (single-stage power-line filter)	55

Figure 32. EMI Current on Power-Line Outside the Cabinet (single-stage power-line filter)	57
Figure 33. EMI current on power line outside the cabinet (two-stage power-line filter)	58

I. INTRODUCTION

A. MOTIVATION FOR THIS THESIS

The performance of receiving sites is often limited because of Electromagnetic Interference (EMI). This interference is often caused by digital devices such as automatic digital telephone switching systems, printers, personal computers etc. When these systems operate, they generate electromagnetic waves rich in spectral content (frequency components) causing interference or noise. Interference can also be caused by external noise sources.

Internally-generated interference travels from its source to a system by a variety of conducted, inductive, and capacitive paths. Radiated interference is received as undesirable electromagnetic (EM) energy by antennas. Conducted interference is injected into receivers by leakage paths associated with poor compartment shielding, grounds, or cable shielding.

An electronic system that is able to function compatibly with other electronic systems and not produce or be susceptible to interference is said to be electromagnetically compatible with its environment.

B. OUTLINE OF THE PROBLEM

Among the different techniques that have been developed to reduce the effects of EMI on sensitive electronic equipment, one technique known as the topological control of EMI has been the most successful. Either the noise source or the sensitive equipment is placed inside an enclosed electromagnetic shielded barrier. By using this method both radiated and conducted interference is reduced to harmless levels.

C. OVERVIEW OF THE THESIS

In this thesis the characteristics of EMI produced by the MITEL SX-20 automatic digital telephone switching system will be examined in the following steps:

- Determination of EMI levels inside the frequency band of interest under various operating conditions.
- Elimination of EMI to receivers and sensitive equipment by suppressing the conducted EMI current levels to magnitudes less than 2 microamperes.

Chapter II gives the theoretical background needed to understanding the different kinds of noise especially those caused by switching systems.

Chapter III describes the implementation of an integrated barrier, filter and ground (BFG) plan. Chapter IV describes the experimental set up, test procedures and instrumentation. It also describes the MITEL SX-20 automatic digital telephone switching system. Chapter V has measurements of EMI current levels over the Radio Frequency (RF) band for the unmodified MITEL SX-20. In Chapter VI measurements are taken after the MITEL SX-20 automatic telephone switching system has been attached to an electromagnetically shielded barrier. Finally, Chapter VII concludes with a discussion of the benefits of a BFG plan and recommendations about the elimination of EMI to receivers and sensitive equipment.

II. THEORETICAL BACKGROUND AND RELATED WORK

A. EXTERNAL EMI SOURCES

Since the early days of radio and telegraph communications, it has been known that a spark generates electromagnetic waves rich in spectral content (frequency components), and that these waves can cause electromagnetic interference (EMI) or noise in

various sensitive electronic equipment such as radio receivers.

Numerous other sources of electromagnetic emissions such as relays, dc electric motors, personal computers (PC's), uninterruptible

power supplies (UPS's), automatic telephone switching systems, digital

electronic devices, power lines, industrial heating equipment, and fluorescent lights can cause interference. Figure 1 shows EMI created by a fluorescent lamp.

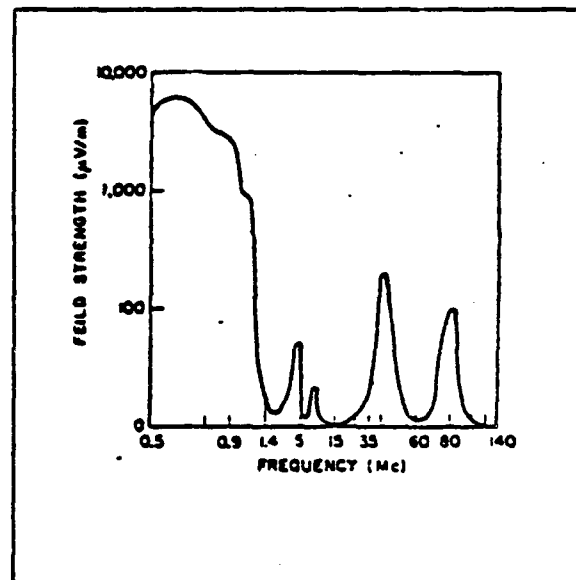


Figure 1. Interference from a Fluorescent Lamp [Ref. 1]

B. INTERNAL EMI SOURCES

Figure 2 lists typical known sources of radio interference. Internal EMI sources are those which originate within a receiver site such as noisy circuit

Broadband			Narrowband	
Transient	Intermittent	Continuous	Intermittent	Continuous
Mechanical Function switches	Electronic computers	Commutation noise	cw-Doppler radar	Power-line hum
Motor starters	Motor speed controls	Electric typewriters	Radio transmitters and their harmonics	Receiver local oscillators
Thermostats	Poor or loose ground connections	Ignition systems	Signal generators, oscillators and other types of test equip- ment	
Timer units	Arc Welding equipment	Arc and vapor lamps	Transponders	
Thyatron trigger circuits	Electric Drills	Pulse generators	Diathermy Equipment	
		Pulse Radar transmitters		
		Sliding contacts		
		Teletype- writer equipment		
		Voltage regulators		

Figure 2. Typical Internal EMI sources [Ref. 9]

components and devices, mixers, local oscillators, digital filters, voltage stabilizers, a wide variety of digital devices, signal generators etc. Depending on the frequency range that their EMI produces, these sources are categorized as broadband or narrowband.

When a receiving site is designed without taking into consideration the EMI present, its ability to receive signals and process data is severely reduced. Electronic systems must be designed ensuring that:

- they don't interfere with other systems
- they are not susceptible to emissions from other systems
- they don't cause interference to themselves

A system that satisfies the above criteria is called electronically compatible.

III INTEGRATED BARRIER, FILTER AND GROUND PLAN

A. TOPOLOGICAL APPROACH

Among the techniques developed to ensure compatibility, the one that has proven to be the most successful at reducing both conducted and radiated EMI effects on sensitive equipment is to place either the noise source or the equipment inside an electromagnetically shielded barrier. This technique is known as the topological approach to the control of EMI. The topological approach uses an integrated Barrier, Filter and Ground (BFG) configuration for the reduction of the effects of EMI over a wide frequency range. The control of EMI is obtained in two ways:

- EMI/RFI generated by equipment within the barrier doesn't leave the enclosure
- EMI/RFI generated by external equipment doesn't enter the enclosure

Figure 3 illustrates an example of a BFG configuration where the noise source is a UPS.

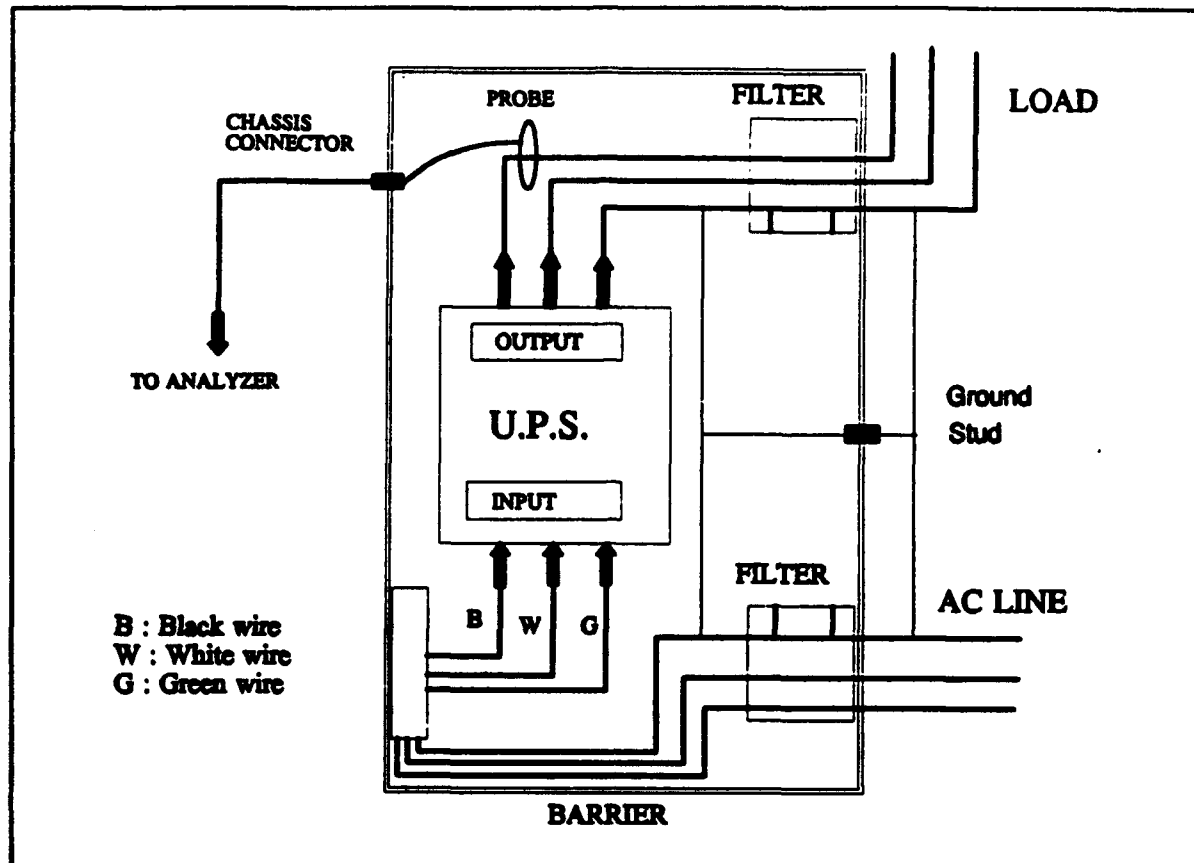


Figure 3. Barrier, Filter and Ground (BFG) Configuration for a UPS

B. BARRIER

The barrier is designed in a such way as to achieve broadband electromagnetic separation between the source of interference and the equipment to be protected. This barrier is a conductive enclosure which shields the equipment of interest. The attenuation of an electromagnetic wave by a metallic barrier is shown in Figure 4. The term barrier is used because

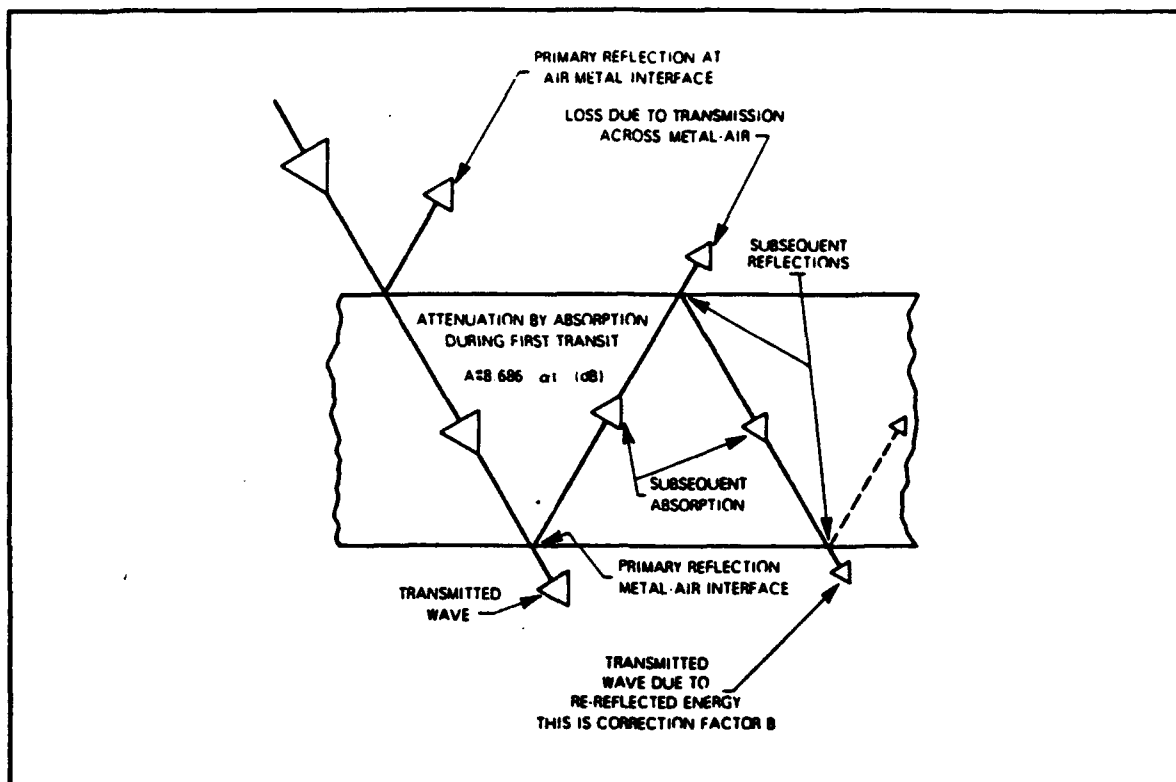


Figure 4. Attenuation of an Electromagnetic Wave by a Metallic Barrier
 [Ref. 1]

of the need to control the EMI/RFI current flowing on all conductors penetrating the cabinet walls. The dimensions of the cabinet are selected to ensure that all paths for EMI currents are small in wavelength. All conductors that penetrate the cabinet must be shielded. Bulkhead connectors must be used at the surface of the enclosure. Ideally a solid enclosure is used. This is obtained by means of conductive gaskets to fill cracks. Other openings in the cabinet are required for control shafts, power and signal

leads, fuse holders, meters, phone jacks, and antennas connectors. Figure 5 shows typical shielded enclosure discontinuities.

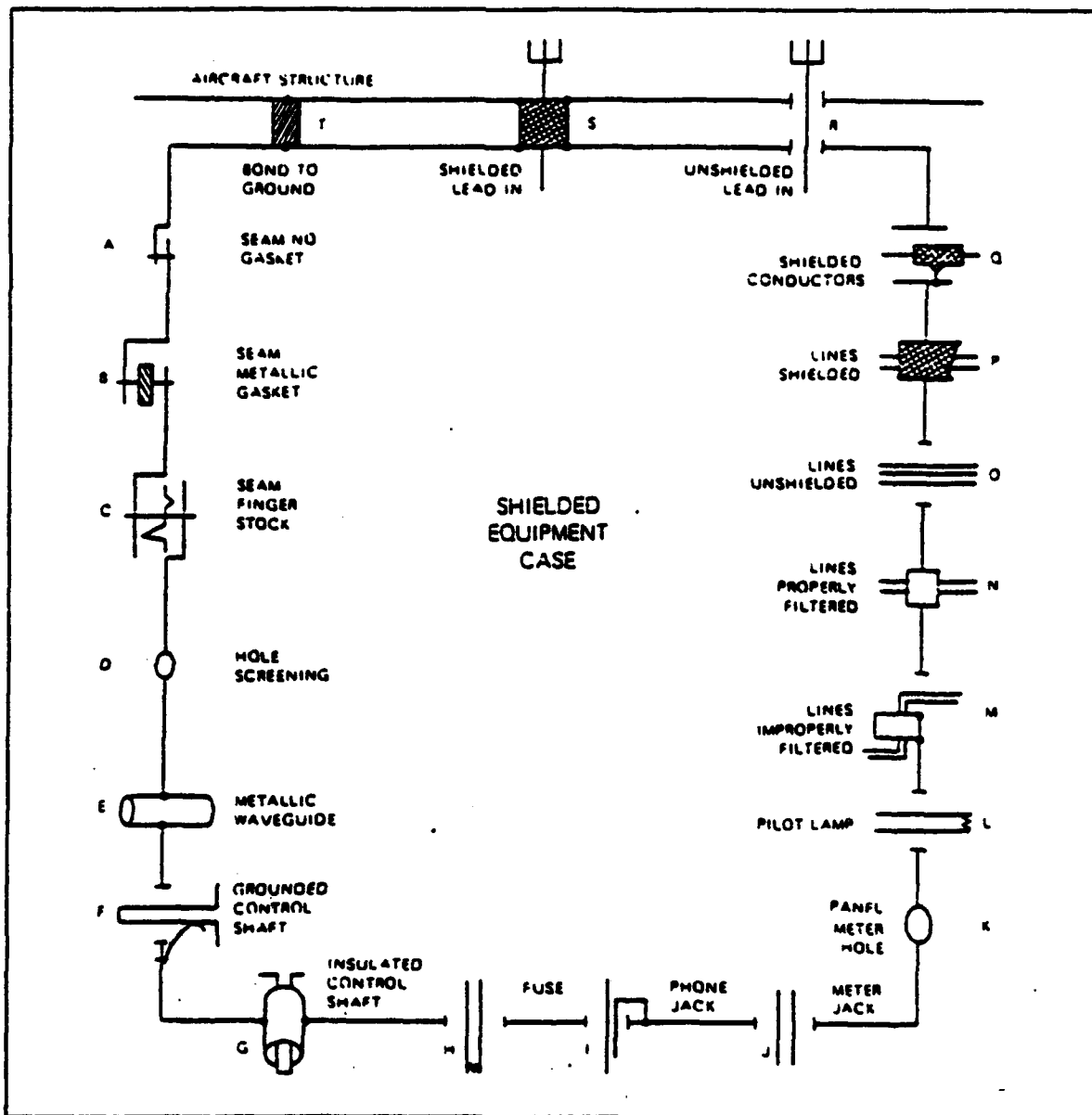


Figure 5. Typical Shielded Enclosure Discontinuities [Ref. 1]

C. FILTERS

In order to prevent EMI/RFI current from flowing across the barrier through power lines, low-pass power-line filters are used. Figure 6 shows three idealized power-line filter configurations, designed to prevent the flow

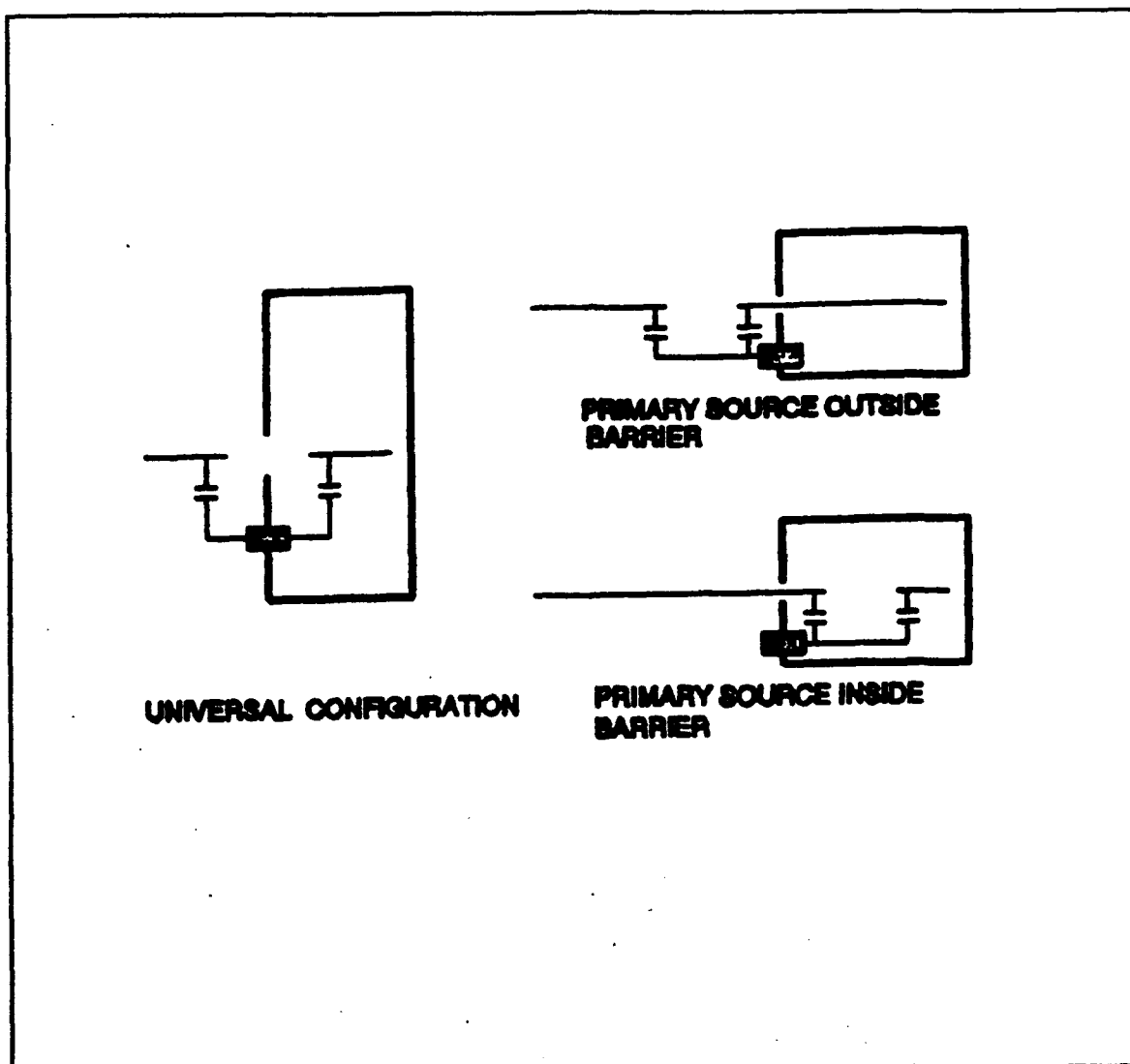


Figure 6. Power-Line Filter Configurations [Ref.5]

of EMI/RFI current across a barrier. Power-line filters must always be installed on a barrier surface. Low-pass signal-line filters are also used. These filters allow desired signals to enter or leave an enclosure while preventing EMI currents from entering or leaving. The above filters must meet the following requirements:

- low-impedance path for the return of externally generated EMI/RFI current
- high impedance path to inhibit the flow of EMI/RFI current across the barrier and into the controlled space. [Ref. 5]

D. GROUNDING

The primary purpose of grounding is for equipment and personnel safety. A secondary purpose is to provide a reference plane for voltages and currents at low frequencies, where the dimensions of the ground system are much less than the wavelength of signals and noise on the reference plane. That means, a reference plane for a signal is provided when the distance between grounding points is less than one-tenth ($<\lambda/10$) of the wavelength. Common signal and power grounds must be avoided.

Ground cables are connected to barriers by use of ground studs. A ground stud is used to bond the exterior surface of the barrier, and the

interior ground to the interior surface of the barrier. The installation of a ground stud, which is in direct contact with the internal and the external surfaces of the enclosure provides:

- A path for internally generated EMI/RFI current to return to its source without exiting the controlled space.
- A return path for externally generated noise current to return to its source without penetrating into the controlled space.

Figure 7 shows how ground penetrations must be done by using ground studs.

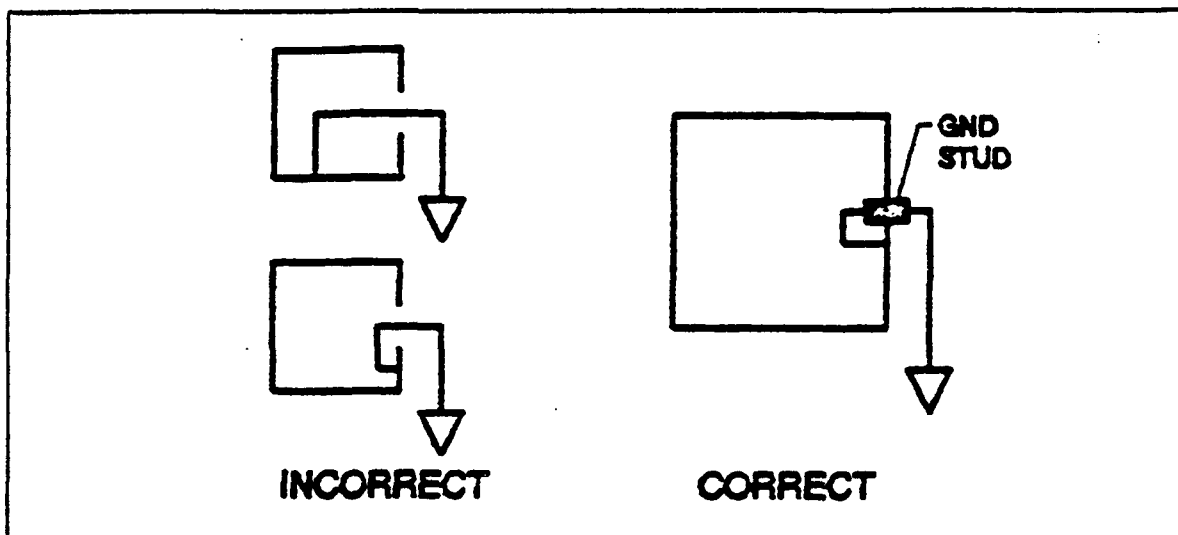


Figure 7. Good and Bad Ground Penetrations [Ref. 5]

IV. EXPERIMENT IMPLEMENTATION

A. GENERAL CONSIDERATIONS

1. Time

The analysis of the effects of EMI current on the performance of receiving sites would be simplified if noise could be modelled as a stationary process. But, about eighty percent (80%) of present-day cases of EMI is a non-stationary process. This means that measurements are highly time dependent. At any particular time, the conducted or radiated EMI currents which travel in power wires and other conductors are primarily related to the intermittent operation of electronic equipment operating in the area. The noise observed on building power and other conductors during working hours is expected to be higher than the noise during non-working hours. This is simply because more equipment is drawing power and injecting noise into the building conductors during working hours.

2. Ambient noise

In the Microwave Laboratory (Spanagel Hall, Room 419) where most of the measurements were made, many electrical loads such as copy

machines, laser printers, and digital devices operate during normal working hours. These loads produce EMI currents which travel by conduction along the power conductors of the building and by inductive coupling into conduits and other conductors. Considering that many others loads exist in Spanagel Hall such as power supplies, laser printers, work stations, test equipment, copy machines, fluorescent lights and digital devices in general, efforts were made to take all measurements with about the same ambient noise profile.

B. MITEL SX-20 DIGITAL TELEPHONE SWITCHING SYSTEM

In this thesis the characteristics of EMI current produced by the MITEL SX-20 automatic digital telephone switching system are examined. The MITEL SX-20 switch is a compact digital communication system employing solid-state digital telephone switching and microprocessor control of call processing. The microprocessor can access all areas of the SX-20 system for information or to change the operating state of the equipment.

Figure 8 shows the MITEL SX-20 automatic digital telephone switching system. The SX-20 system consists of a single unit metal chassis, and an impact resistant plastic cover. All connections between the SX-20 system, the distribution frame and the peripherals use 25-pair connectorized cables. The

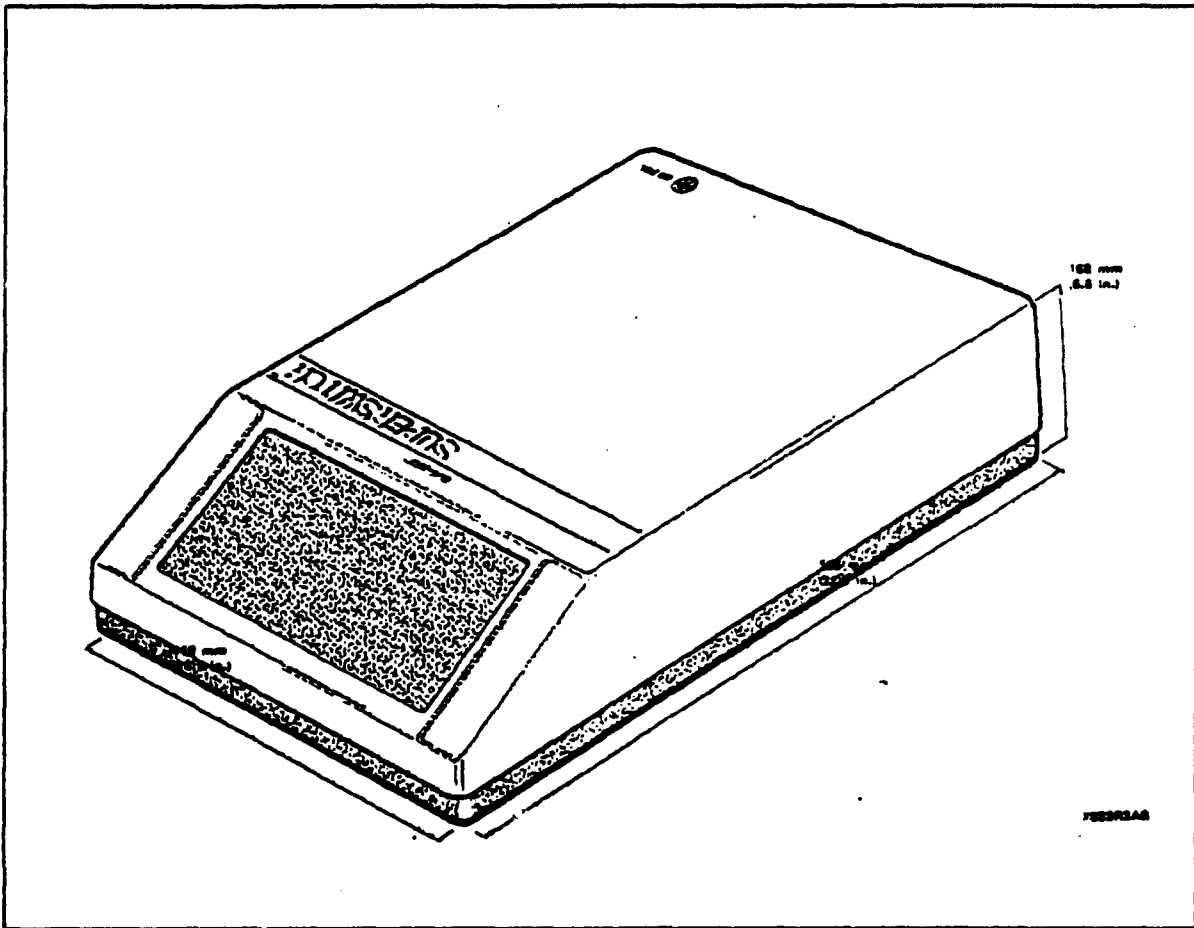


Figure 8. MITEL SX-20 Automatic Digital Telephone Switching System

distribution frame and the peripherals use 25-pair connectorized cables. The overall dimensions of the SX-20 system are 6.6 inches in height, 16.5 inches in width and 22.3 inches in length. The SX-20 system can be wall-or desk-mounted.

1. Chassis

The SX-20 chassis holds the system power supply, the cooling fan, the SUPERSET Connector Card and the equipment backplane. The equipment cards plug into the backplane and are held in position by card retainers. The hinged chassis side panel allows access to the circuit cards for removal and insertion. The chassis is completely enclosed within the lockable equipment case.

2. Printed Circuit Cards

All printed circuit cards employed in the system consist of a fiberglass board with printed circuit patterns on both of their faces. Located on the front edge of the circuit board is an extractor clip which allows the cards to be removed from the equipment chassis. Each of the card types have a keyed connector preventing the card from being plugged into incorrect card slot. In the experiments the following Printed Circuit Cards were used:

- CPU II Card
- Miscellaneous Card
- Superset Line Card

3. Primary Power Supply

The primary power supply for the system is mounted at the rear of the equipment chassis and provides all the system power from a 105-125 Vac, 47-63 Hz input with a maximum current drain of 3 Amperes.

4. Cooling Fan

A cooling fan is mounted at the rear of the cabinet. The fan draws cooling air through a filter mounted at the base of the cabinet and passes it over the circuit boards. The cooling air exits through vents in the side of the cabinet. A temperature sensor protects the circuit cards in the event of a fan failure by automatically disconnecting the power feed.

5. MITEL SUPERSET-3 Telephone Set

In our experiments the SX-20 system was used with a MITEL SUPERSET-3 Telephone Set. The SUPERSET-3 is an advanced microprocessor-controlled telephone set, employing digitally-controlled integrated circuitry. The SUPERSET-3 set was connected to the SX-20 system through a 25-pair connectorized cable. Figure 9 shows the block diagram for the MITEL SX-20 system.

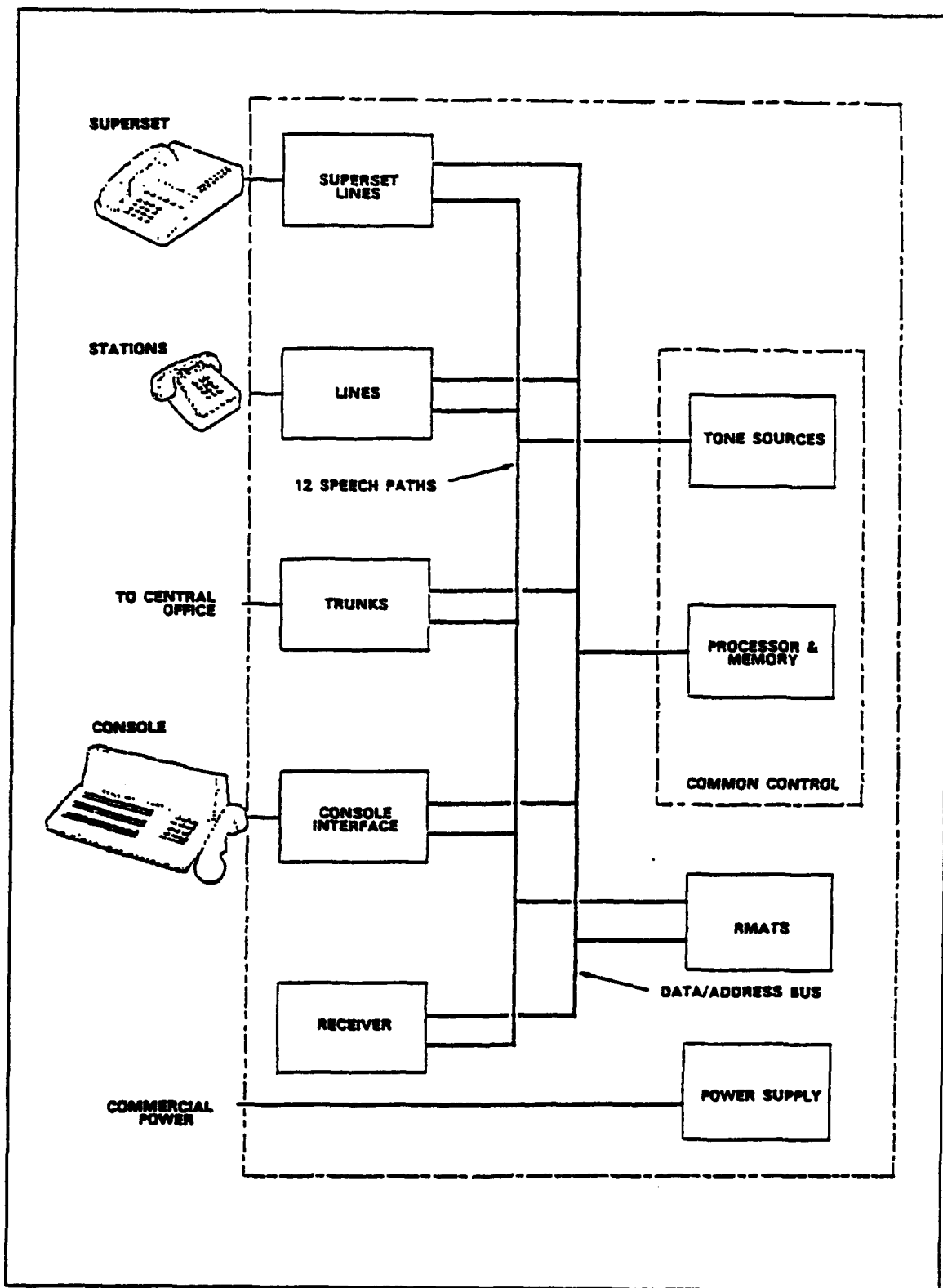


Figure 9. MITEL SX-20 Block Diagram [Ref. 15]

C. INSTRUMENTATION

1. Description

The experiments included measuring EMI current levels on power-line conductors, on ground line conductors and on telephone line conductors. EMI was examined over the frequency range from 0 to 100 MHz. The primary instrumentation used for the experiments included a Develco Model 7200B 3-Axis Display, Hewlett Packard 141T Spectrum Analyzer, Fischer Model F-70 RF Current Probe and selected filters and RF amplifiers.

The 3-axis display provides a unique measuring tool for observing spectral and temporal properties of noise and signals over a period of time. Figure 10 shows an example of stored history of the analyzer output. This display can be frozen with the present and previous scans stored in memory, and the stored view can be oriented for best viewing and signal analysis. The 3-Axis presentation can be photographed for later analysis.

The Hewlett Packard Series 141T Spectrum Analyzer is used as a scanning receiver to allow the observation of signals and EMI current components up to a frequency of 100 MHz. The Fischer Model F-70 RF Current Probe was used to measure current flowing on the conductors. An

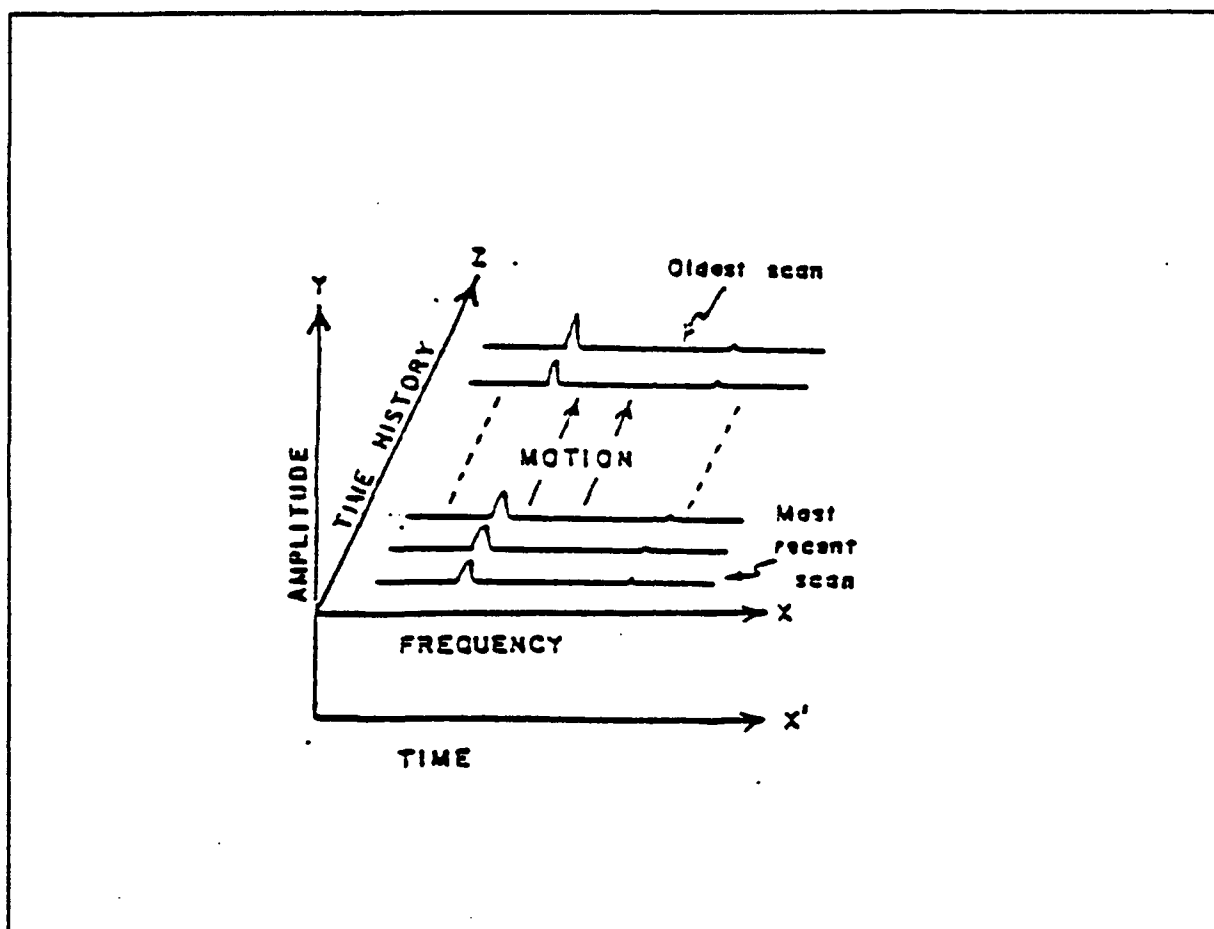


Figure 10. 3-Axis Display [Ref. 4]

RF Amplifier with 20-dB gain was used to amplify the output of the Model F-70 RF Current Probe. All interconnecting signal cables used for the experiments were double-shielded RG-223 coaxial cables. Finally a Tektronics C5 Polaroid camera was used to obtain time-and frequency-domain pictures of EMI current.

2. Unmodified MITEL SX-20 Set-up

Figure 11 shows the setup for the unmodified MITEL SX-20 system. The MITEL SX-20 system was placed on a laboratory bench in the Microwave Lab (Spanagel Hall, Room 419). The primary power on that

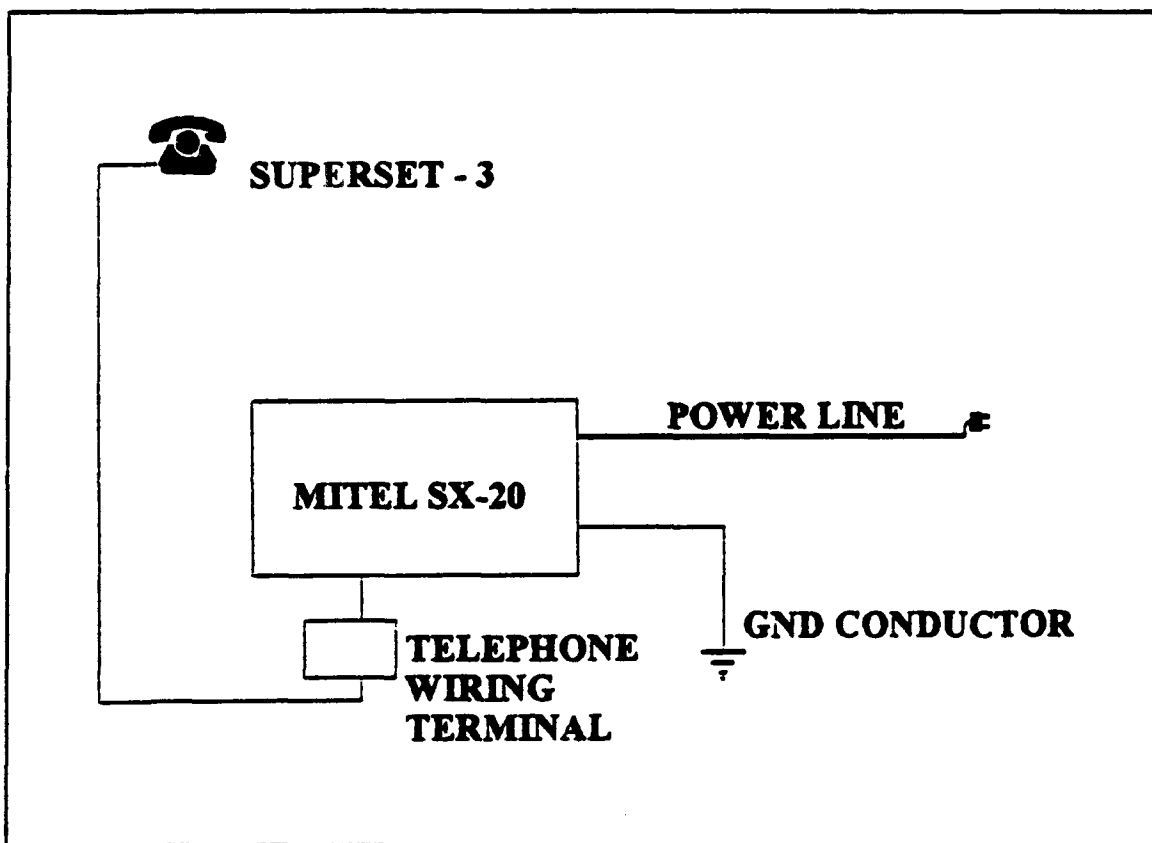


Figure 11. Unmodified MITEL SX-20 Set-Up

bench (120 Vac, 60 Hz) provided electricity to the MITEL SX-20 system and all instrumentation. A ground terminal on the bench was used for the system earth ground. The "male" plug at the end of a 25-pair telephone cable

was attached to the Superset Line Card. The other end of the cable was connected to a telephone wiring terminal. The SUPERSET-3 Telephone Set was then connected to that telephone wiring terminal by means of a 30-foot telephone cable.

Figure 12 shows the data acquisition and processing channel. This channel consists of the Fischer RF current probe whose output was connected to a 20-dB gain RF amplifier. The output of the RF amplifier was fed to 141T Spectrum Analyzer whose output was connected to a Develco

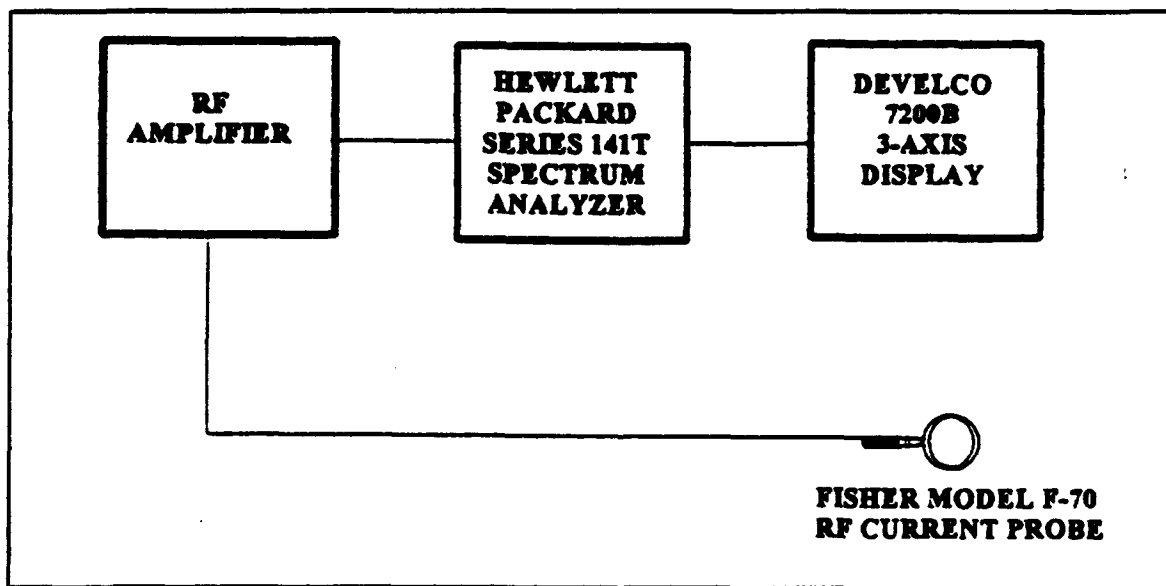


Figure 12. Data Processing Channel

7200B 3-Axis Display. This configuration was used to obtain data with a modest spectral resolution and a high temporal resolution.

3. Modified MITEL SX-20 Set-up

Figure 13 shows the set-up for the modified MITEL SX-20 system. The configuration was based on the topological approach for controlling EMI current as described in Chapter III. Following this method a metal enclosure

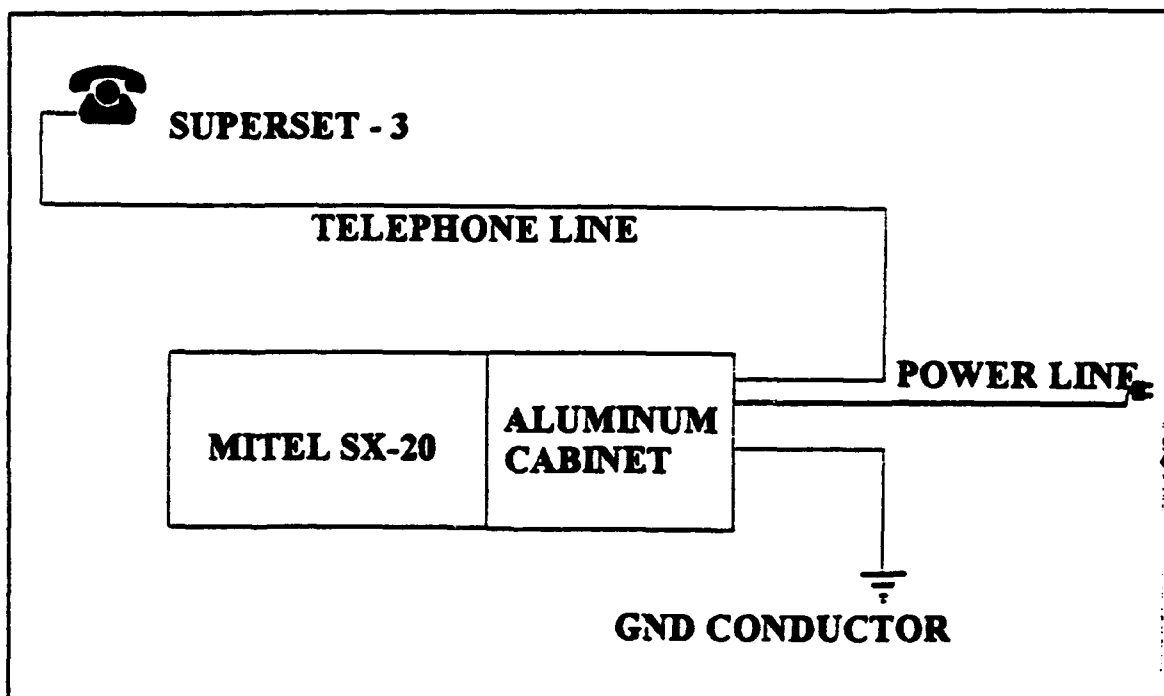


Figure 13. Modified MITEL SX-20 Set-Up

was constructed from soft aluminum to shield the MITEL SX-20 from ambient EMI current and to contain interference emitted by the equipment. This enclosure is the barrier of an integrated barrier, filter and ground (BFG) configuration.

The barrier was attached to the MITEL SX-20 system at its bottom where the power conductors, ground conductor, and telephone-line conductors exited the system as is shown in Figure 14. No uncontrolled conductor was allowed to penetrate the barrier. Two metal-encased low-pass

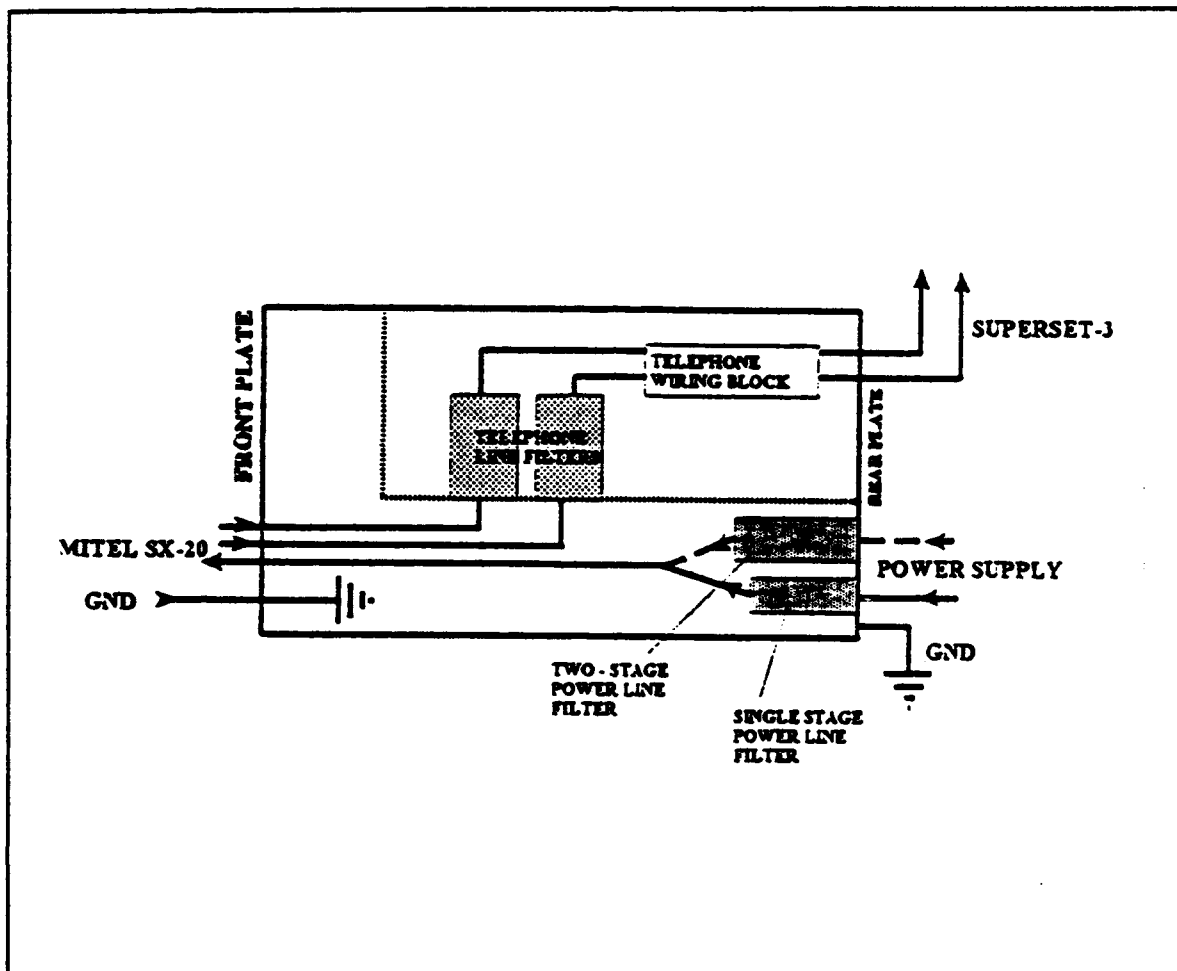


Figure 14. Aluminum Cabinet for MITEL SX-20 System

telephone-line filters were mounted on the separation plate. Two types of power-line filters, terminating at a "male" plug, were mounted through

openings at the rear plate of the cabinet. One power-line filter was a single-stage low-pass unit and the other was a two-stage low-pass unit. Both filters were used.

After mechanical assembly, the enclosure wiring was completed. All the necessary connections were made by soldering or screwing wires to terminal blocks. All wiring strictly followed the topological approach. The permanent power source on the working bench was used to feed the MITEL SX-20 with 120-V, 60-Hz current through the power-line filter located on the surface of the barrier.

V. UNMODIFIED MITEL SX-20 MEASUREMENTS

A. GENERAL APPROACH

Initial measurements on an unmodified MITEL SX-20 showed significant spectral and temporal components of EMI/RFI current on the ground wire, telephone line and power line. These components covered the entire frequency range from 0 to 100 MHz. All pictures of spectral and temporal structure in the following figures are accompanied by a small chart which provides the following information:

- Date, time
- Location, Room, Equipment, Device under test
- Center frequency, Frequency span, IF Bandwidth, Scan time
- Probe identification, Amplification gain, RF Attenuation, Reference level

Only the date and time appears in some picture. This means that the information in that picture is the same as in a prior picture with the same date and time. Because of the presence of significant noise components in some particular frequency regions, expanded frequency spans were selected

to obtain clearer and more detailed views of the temporal and spectral structure of the EMI current.

B. GROUND CABLE MEASUREMENTS

EMI/RFI current in the ground cable was measured over a frequency band of 0 to 100 MHz (see Figure 15), and from 0 to 20 MHz (see Figure 16). Current values were used to determine the amount of EMI (and eventually noise power) generated by the MITEL SX-20 over these frequency ranges. The estimated EMI noise power provides information for the amount of total power that must be dissipated in the filter portion of the BFG configuration.

Figure 15 shows that the entire frequency range from 0 to 100 MHz is contaminated by noise. The amplitude vs. current picture shows that large EMI/RFI current components exist at a center frequency of 5 MHz with an amplitude of about 9 microamperes. The next significant components appear near a center frequency of 15 MHz, also with an amplitude of about 9 microamperes. The frequency range from 25 to 30 MHz is covered by noise components with an average amplitude of about 7 microamperes. Noise in

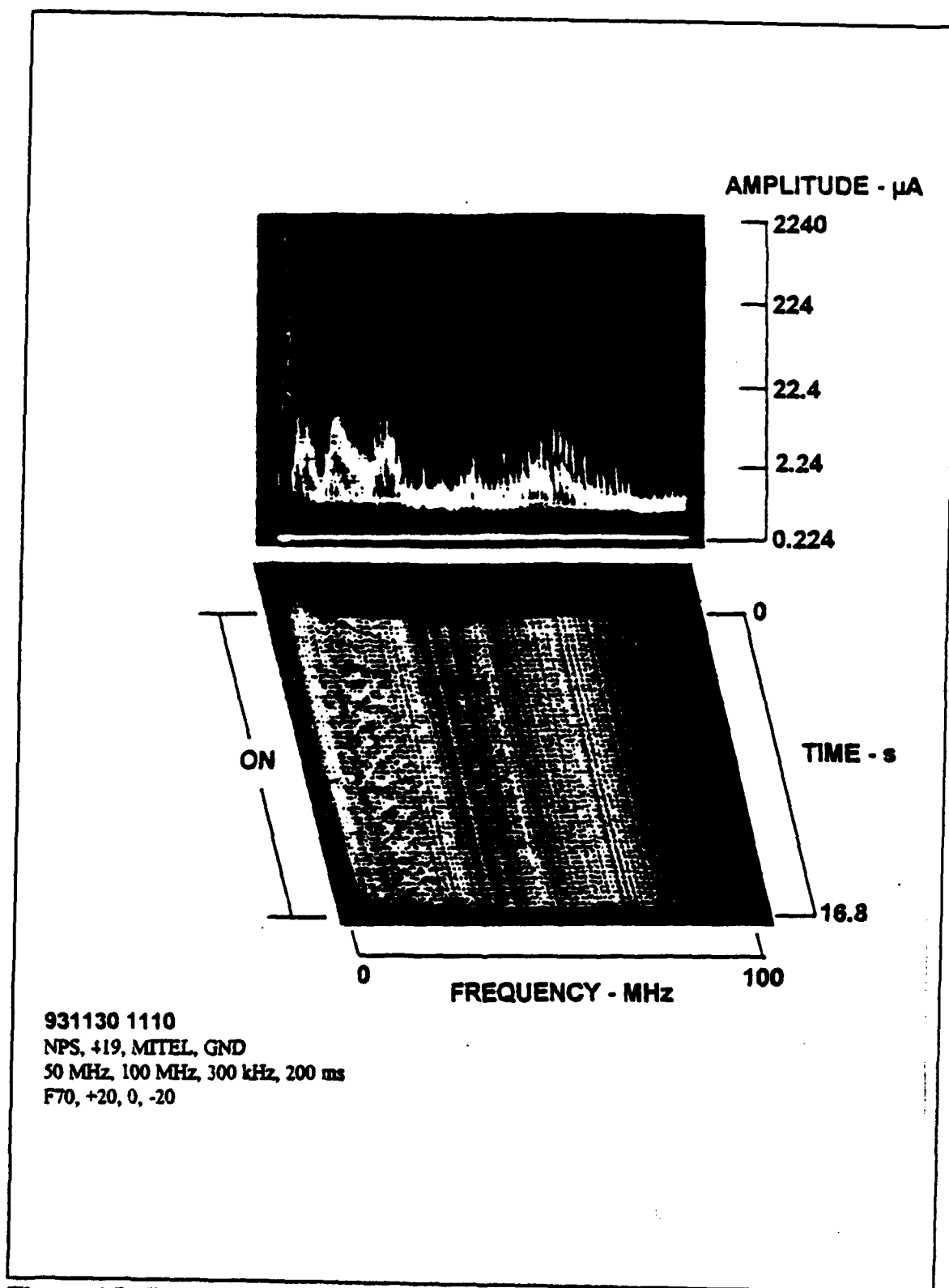
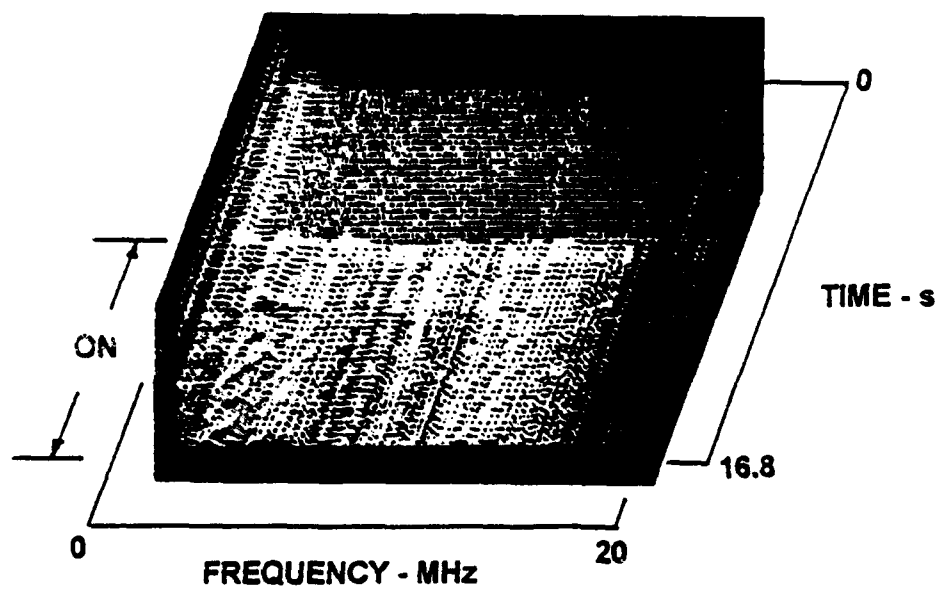


Figure 15. EMI Current on MITEL SX-20 Ground Cable

frequency range from 30 to 100 MHz was found with a peak of 6 microamperes at about 70 MHz. The most significant components of EMI/RFI current were found in the frequency range from 0 to 20 MHz. For this reason the frequency span is expanded in Figure 16 to provide an improved view of the strongest spectral components. Figure 16 also shows the transient response and the spectral structure when the MITEL SX-20 is turned on during warm-up, and during normal operation.

Figure 17 shows amplitude vs. frequency views of the same data shown in Figure 16. The observation time is divided into three parts (ambient noise before turn on, warm up, and normal operation) and Figure 17 shows the frequency response for each one. In the top picture in Figure 17, only the ambient noise floor observed by the instrumentation is shown. The middle picture shows the frequency response as the MITEL SX-20 is turned on. EMI/RFI current appears which covers almost the entire frequency range. Local peaks appear at 1.3 and 5 MHz with amplitudes of about 8 microamperes. Another peak appears at 15 MHz with an amplitude of about 7 microamperes. The bottom picture in Figure 17 shows the frequency response under steady state condition. EMI/RFI components were found at the same frequencies at slightly lower amplitudes.



931130 1115
NPS, +19, MITEL, GND
10 MHz, 20 MHz, 30 kHz, 200 ms
F70, +20, 0, -30

Figure 16. Ground Cable Transient Response

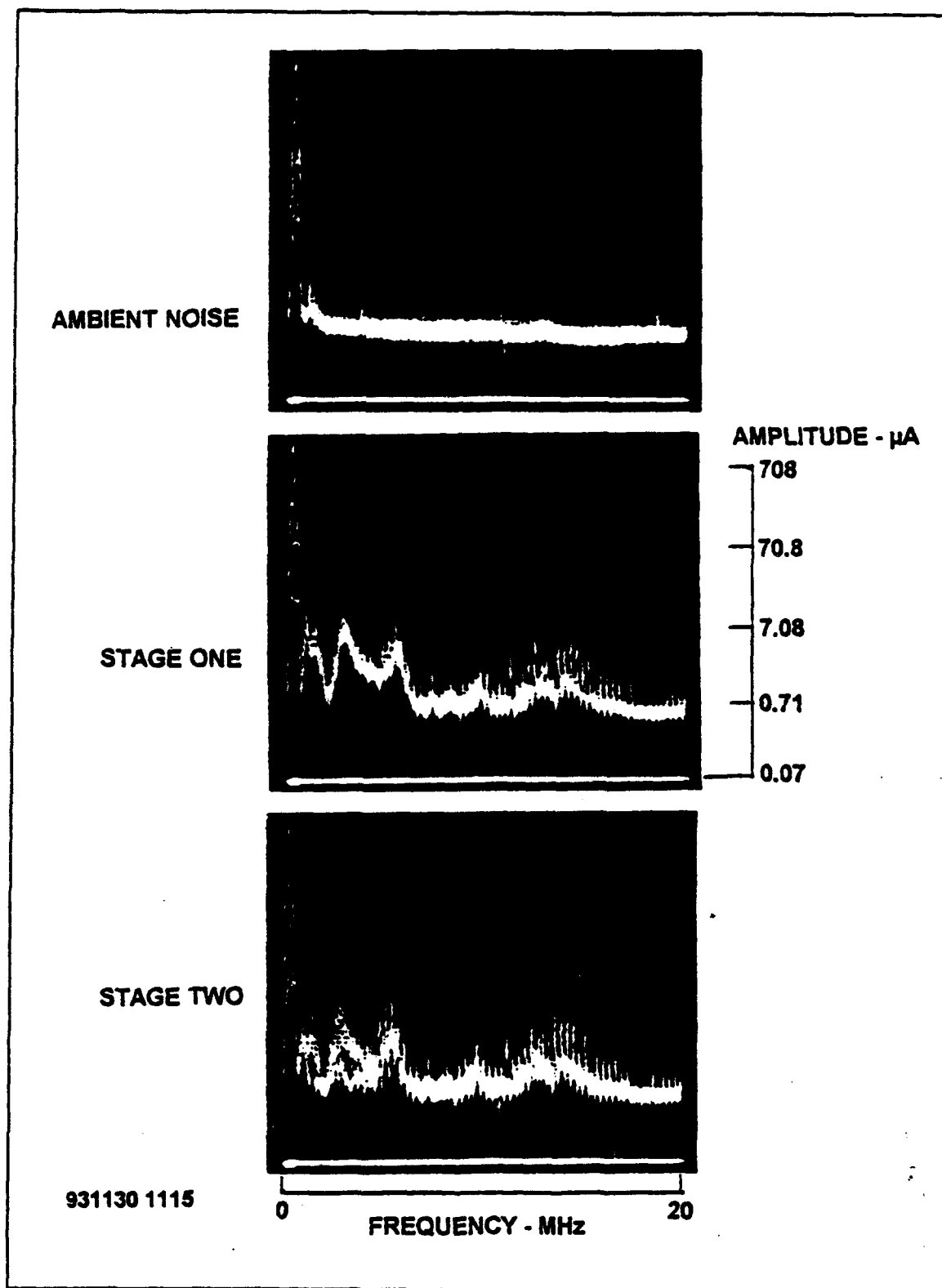
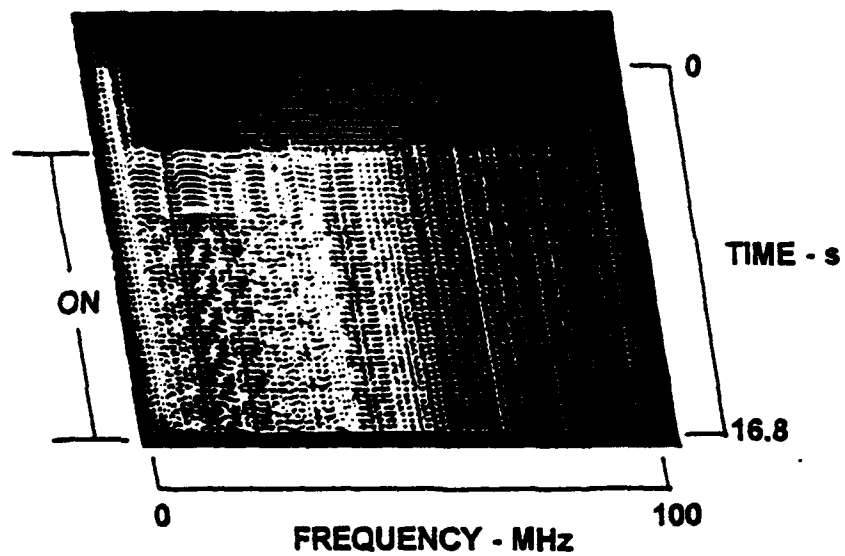


Figure 17. EMI Current on MITEL SX-20 Ground Cable

C. TELEPHONE LINE MEASUREMENTS

The MITEL SUPERSET-3 telephone system was connected to MITEL SX-20 main unit with a 30-foot long standard telephone wire. The current-clamp was placed 1 foot away from the main unit. Figure 18 shows the 3-axis view of the telephone-line EMI response when the MITEL SX-20 was turned on. The observation time was 16.8 seconds and was obtained over a frequency range of 0 to 100 MHz. The distinct changes in the EMI current at turn on and during normal operation are shown in the 3-axis time-history view.

Figure 19 shows the spectral structure of the EMI current on the ground conductor during the three parts of the start-up period. The top picture in Figure 19 shows the floor noise of the instrumentation and it is generally free from ambient EMI/RFI current. The middle picture in Figure 19 ("STAGE ONE") shows the frequency response at the time when the MITEL SX-20 is turned on. The EMI/RFI current almost covers the entire band. Interesting noise peaks appear at the lower part of the spectrum from 0 to 25 MHz with amplitudes of about 14 microamperes.



931130 1200
NPS, +19, MITEL, TELEPHONE LINE
50 MHz, 100 MHz, 300 kHz, 200 ms
F70, +20, 0, -30

Figure 18. EMI Current on MITEL SX-20 Telephone Line

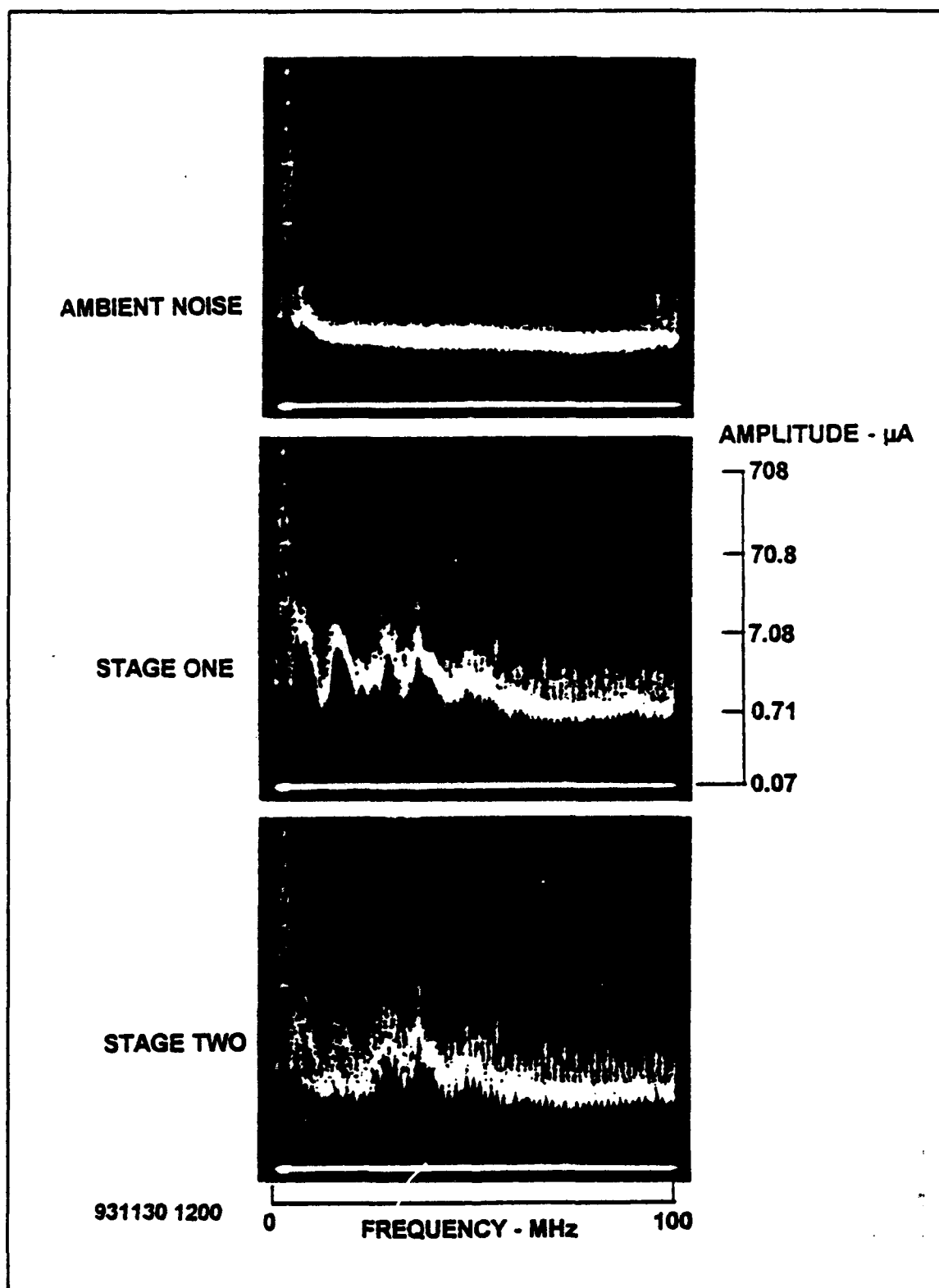


Figure 19. EMI Current on Telephone Line during Turn-On

The bottom picture in Figure 19 ("STAGE TWO") shows the frequency response of the steady-state condition during normal MITEL SX-20 operation. Again the entire spectrum is covered by EMI/RFI components with an average "floor" level of about 3 microamperes. Large components appeared in the lower part of the spectrum from 0 to 30 MHz with amplitudes of about 12 microamperes.

Figure 20 shows the frequency response of current flowing on the telephone line after 10 minutes of operation. The bottom picture in Figure 19 ("STAGE TWO") can be compared with the amplitude-vs.-frequency view in Figure 20. The noise components during normal operation remain about the same over a long period of time. A few stronger components are found at the lower part of the frequency range.

Figure 21 provides a more detailed view of the spectral and the temporal structure of EMI current at the lower part of the spectrum by showing a frequency span of 0 to 20 MHz at a scan time of 100 milliseconds. The MITEL SX-20 operates under steady-state condition for this view. Slanting lines of noise appear at the 3-axis view in Figure 21 which are from impulses synchronized to the power-line frequency. These impulses are generated by the power supply of the MITEL SX-20 system.

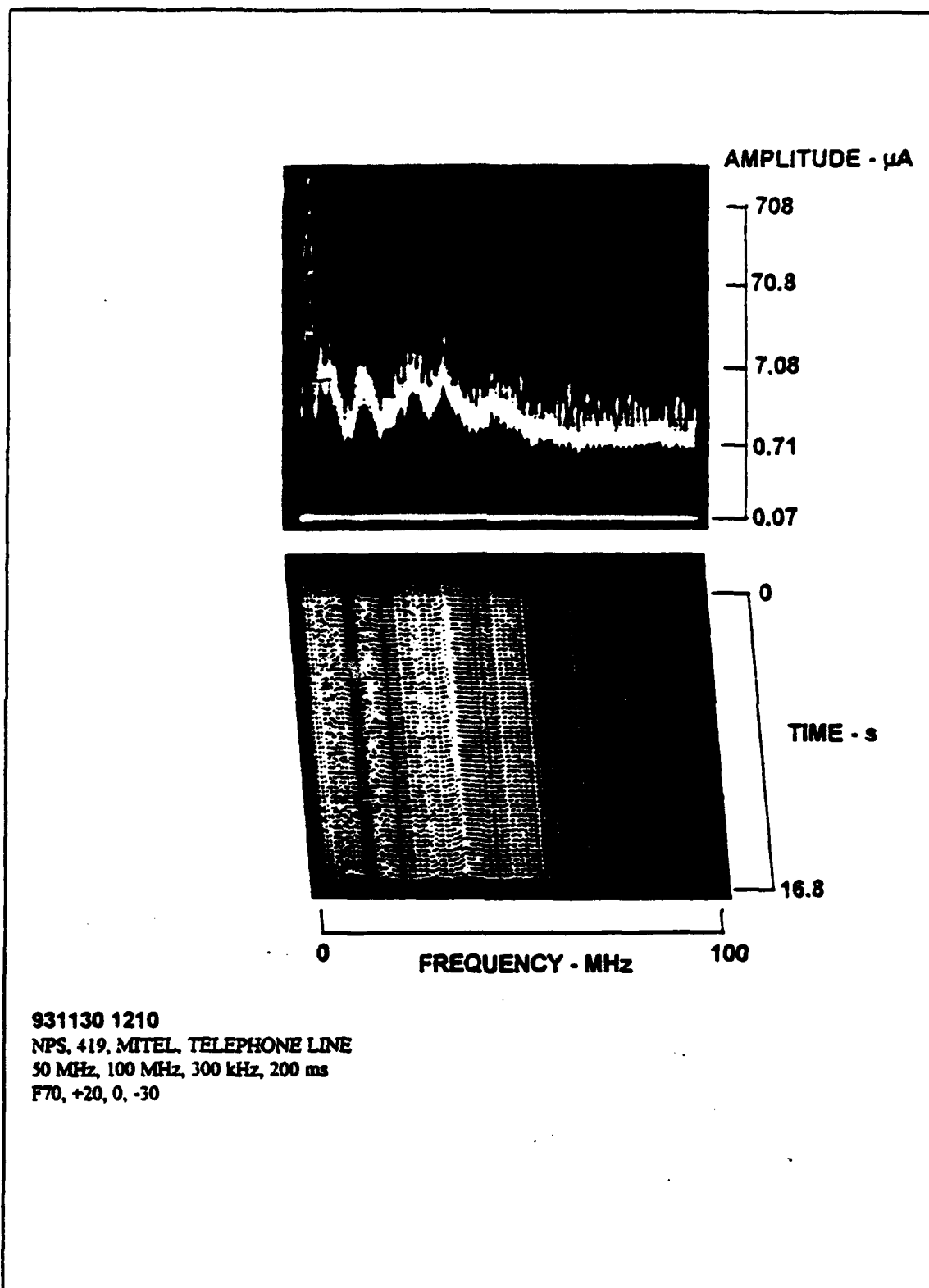


Figure 20. EMI Current on MITEL SX-20 Telephone Line

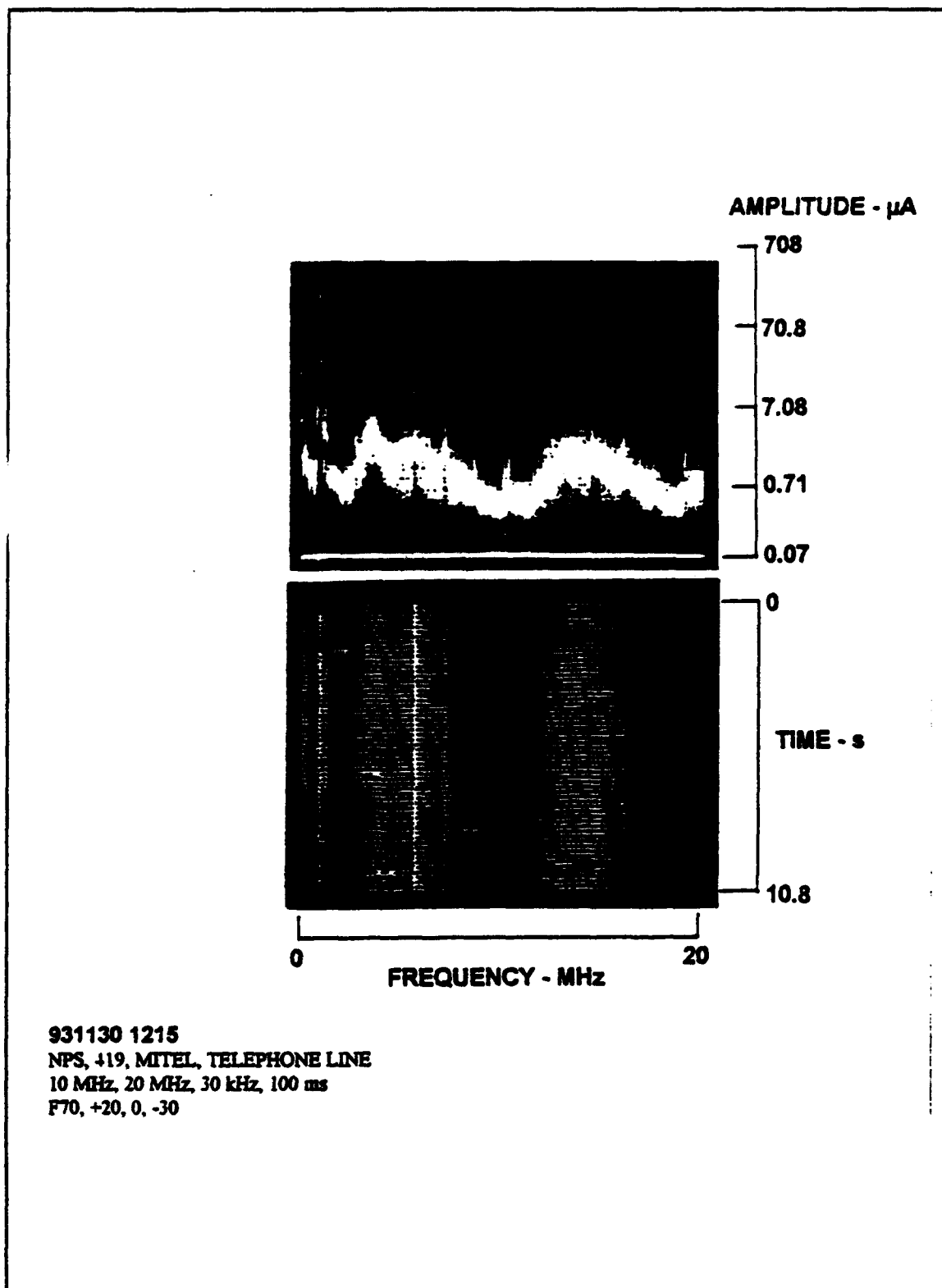
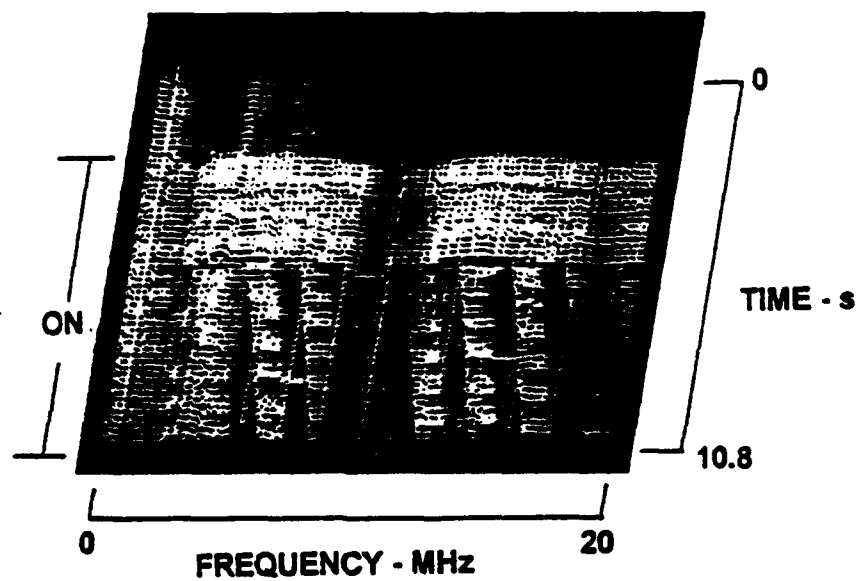


Figure 21. Slanting Lines of Noise on MITEL SX-20 Telephone Line

Figure 22 shows the 3-axis view of the transient response of EMI current on the telephone line when the MITEL SX-20 is turned on. The frequency span is from 0 to 20 MHz, the scan time is 100 milliseconds, and the observation time is 10.8 seconds. The slanting lines of noise in Figure 21 have the same separation and slope as those in Figure 22 which indicates that the period between bursts of noise hasn't changed.

In Figure 23 the observation time was divided into three parts and the spectral response for each is shown separately. The top picture in Figure 23 shows the spectral response of the ambient noise on the telephone line before the MITEL SX-20 was turned on. No EMI/RFI current appeared at this time. Only low-level ambient noise from other sources in the building are shown.

The middle picture in Figure 23 ("STAGE ONE") shows the frequency response of the EMI current on the telephone line when the MITEL SX-20 is turned on. Excess EMI/RFI current is shown. Maximum levels of EMI current were found from 2 to 8 MHz with a peak value of about 14 microamperes. Additional noise components appeared from 12 to 18 MHz with a peak amplitude of about 12 microamperes.



931130 1220
NPS, 419, MITEL, TELEPHONE LINE
10 MHz, 20 MHz, 30 kHz, 100 ms
F70, +20, 0, -30

Figure 22. Telephone Line Transient Response

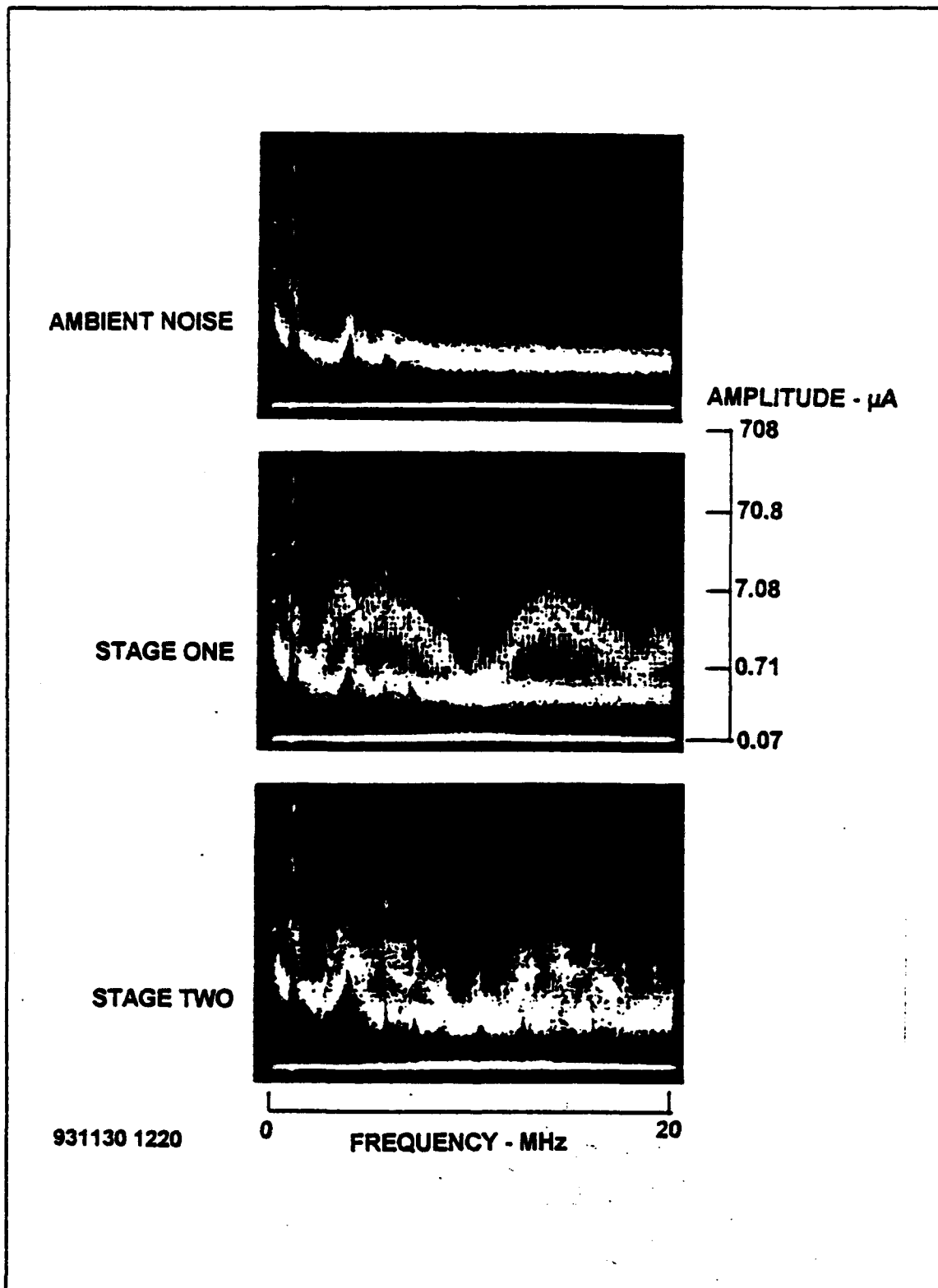


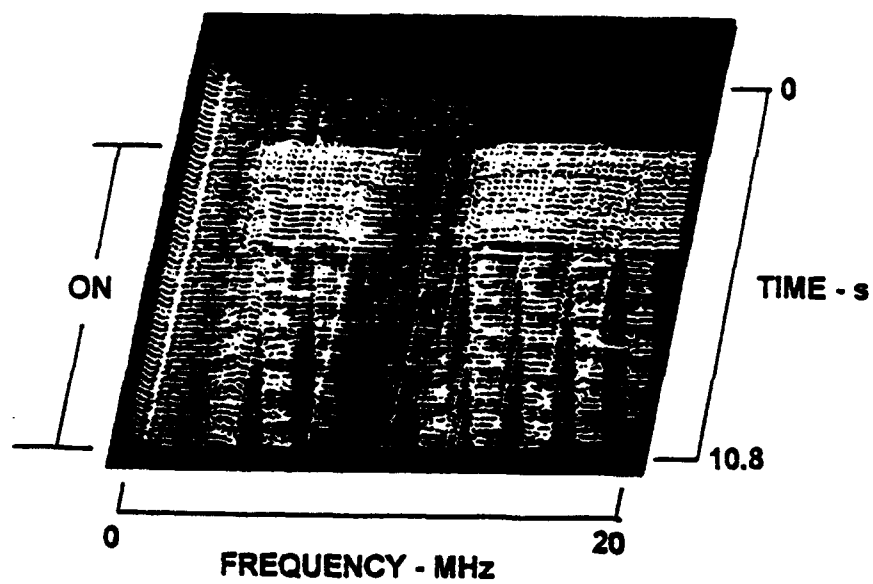
Figure 23. EMI Current on MITEL SX-20 Telephone Line

The bottom picture in Figure 23 ("STAGE TWO") shows the frequency response of the telephone line under MITEL SX-20 steady-state operation. The EMI/RFI current continues to cover almost the entire frequency range. The maximum noise levels were found in the frequency band from 2 to 8 MHz with a peak amplitude of about 12 microamperes. In the frequency range from 12 to 18 MHz, noise components also appeared with a peak amplitude of about 10 microamperes.

D. POWER LINE MEASUREMENTS

Figure 24 shows the 3-axis view of EMI current flowing on the power line. The current clamp was placed six inches from the main unit. The center frequency is 10 MHz resulting in a frequency span of 0 to 20 MHz. The time of the observation is 10.8 seconds. The amplitude of the noise increased significantly at the time when the MITEL SX-20 was turned on. The slanting lines of the temporal structure of the noise are also visible in the same picture during phase II of the turn-on.

In Figure 25 the observation time was again divided into three parts. The three views in Figure 25 show the frequency response of EMI flowing on the power line for each part of the turn-on sequence. The first picture in



931130 1400
NPS, 419, MITEL, POWER LINE
10 MHz, 20 MHz, 30 kHz, 100 ms
F70, +20, 0, -30

Figure 24. Power-Line Transient Response

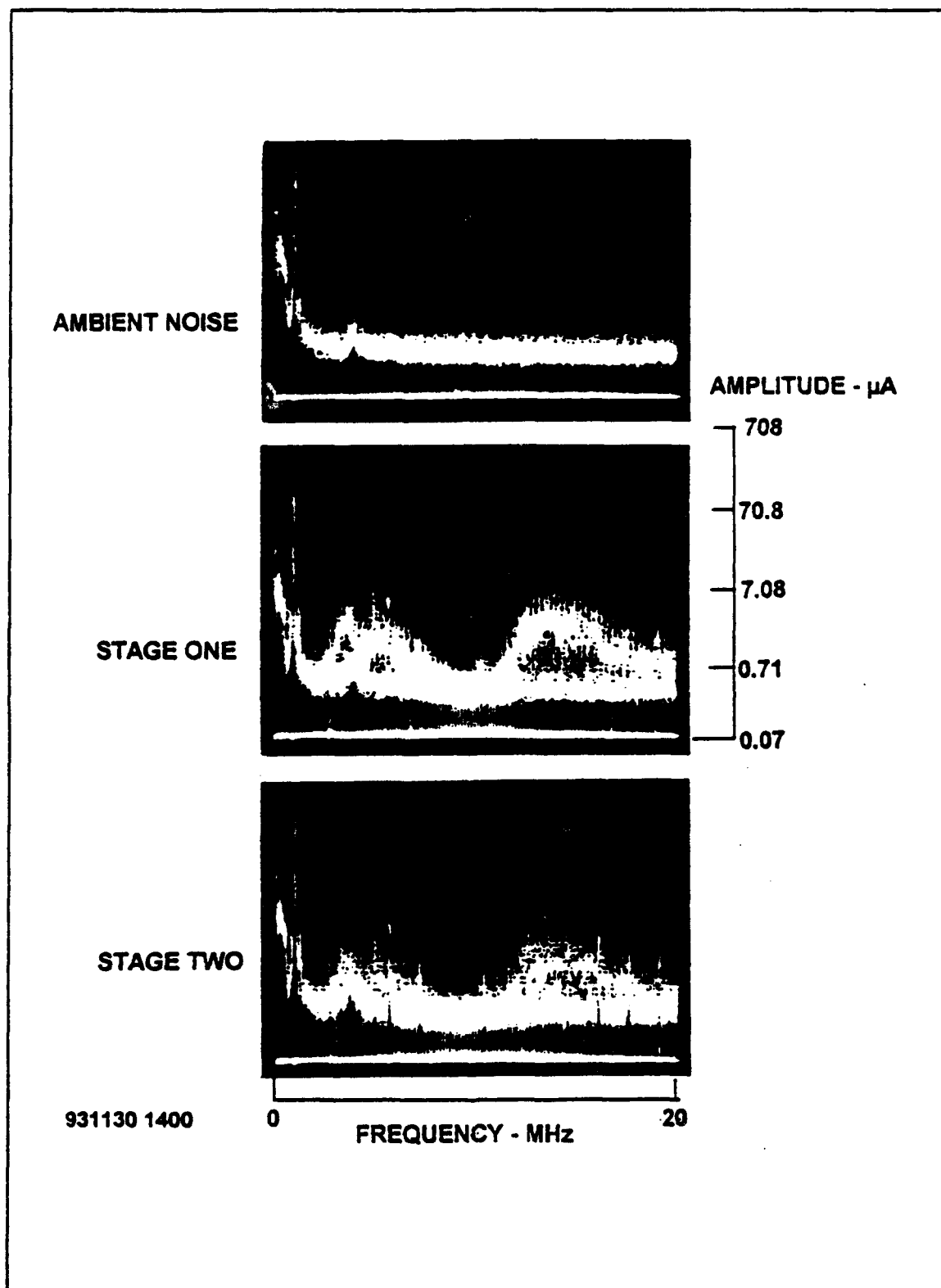


Figure 25. EMI current on MITEL SX-20 power-line

this Figure shows the ambient EMI noise on the power line over a frequency range from 0 to 20 MHz prior to turn-on. Significant EMI/RFI components were not found. This view shows that the power supply line is almost free of noise.

The next picture in Figure 25 ("STAGE ONE") shows the frequency response of EMI current on the power line at the time when the MITEL SX-20 is turned on. Excess EMI/RFI current appeared immediately at turn-on. This noise is injected into the power line by the MITEL SX-20. High amplitude EMI/RFI components appeared from 3 to 9 MHz with a peak amplitude of about 12 microamperes. From 9 to 12 MHz the noise amplitude is reduced to a level of 0.7 microamperes. Then, from 12 to 19 MHz EMI/RFI current is appeared again with a peak value of about 12 microamperes. Clearly the MITEL SX-20 is injecting excessive EMI/RFI current into the power supply line during its operation.

VI. MODIFIED MITEL SX-20 MEASUREMENTS

A. GENERAL CONSIDERATIONS

Measurements on the modified MITEL SX-20 provided another set of data on the spectral and temporal structure of EMI current on the ground cable, telephone line, and power-line. Most measurements were made over a frequency range of 0 to 20 MHz. This range was selected because large EMI current components generated by the MITEL SX-20 system, as is shown in chapter V, are concentrated within these frequencies.

The same measurement and data processing equipment used to obtain data in chapter V was also used for the measurements on the modified MITEL SX-20 system. The data was recorded by the same Tektronics C5 Polaroid camera. The ambient noise during these measurements was about the same as that encountered during measurements on the unmodified MITEL SX-20 system.

B. GROUND CABLE MEASUREMENTS

EMI current levels were measured on the ground conductor of the modified MITEL SX-20 system over a frequency band of 0 to 20 MHz as

shown in Figures 26 and 27. The amplitude of EMI current on the modified system can be compared with the uncontrolled configuration (see figures 15, 16, and 17), to derive measure of the effectiveness of the topological approach to the control of EMI.

Figure 26 shows the EMI current flowing on the ground conductor inside the enclosure. The frequency range was 0 to 20 MHz and the duration of the measurement was 16.8 seconds. At about 5 seconds the MITEL SX-20 system was turned on. EMI currents components appeared but just slightly above the ambient noise. These EMI currents were spread over the entire frequency band, with a "flat" amplitude of about 2 microamperes. This current was considerably lower than that obtained for the unmodified system. Apparently the surface of the enclosure provided an internal return path for some of the ground current.

In Figure 27 the current-clamp was placed on the ground lead outside the barrier. The observation time was again 16.8 seconds and the frequency range was 0 to 20 MHz. The MITEL SX-20 system was turned on at about 5 seconds. The absence of EMI current is obviously shown in this Figure. All EMI current is below the ambient noise level, of about 0.7 microamperes.

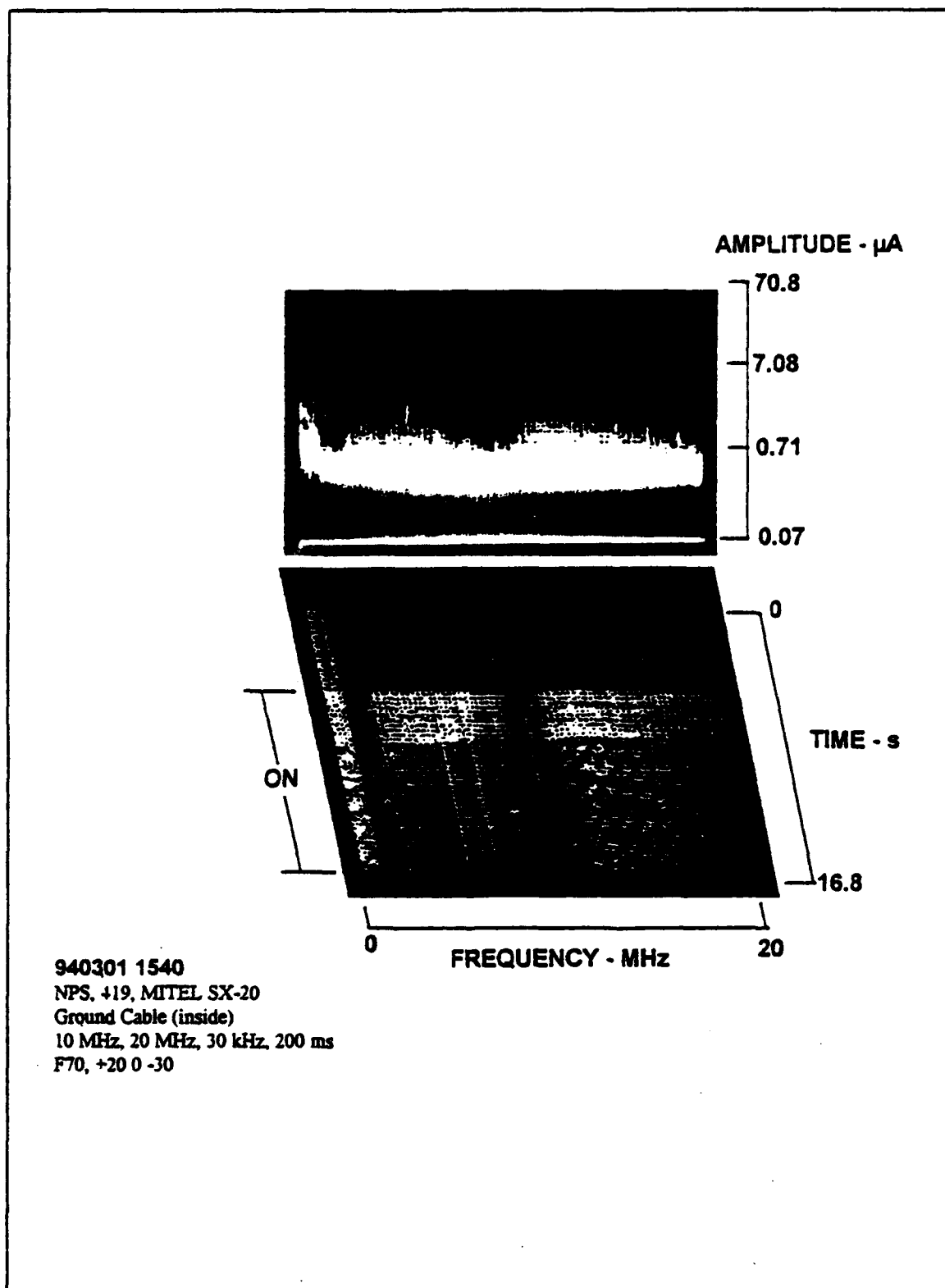


Figure 26. EMI Current on Ground Cable Inside the Cabinet

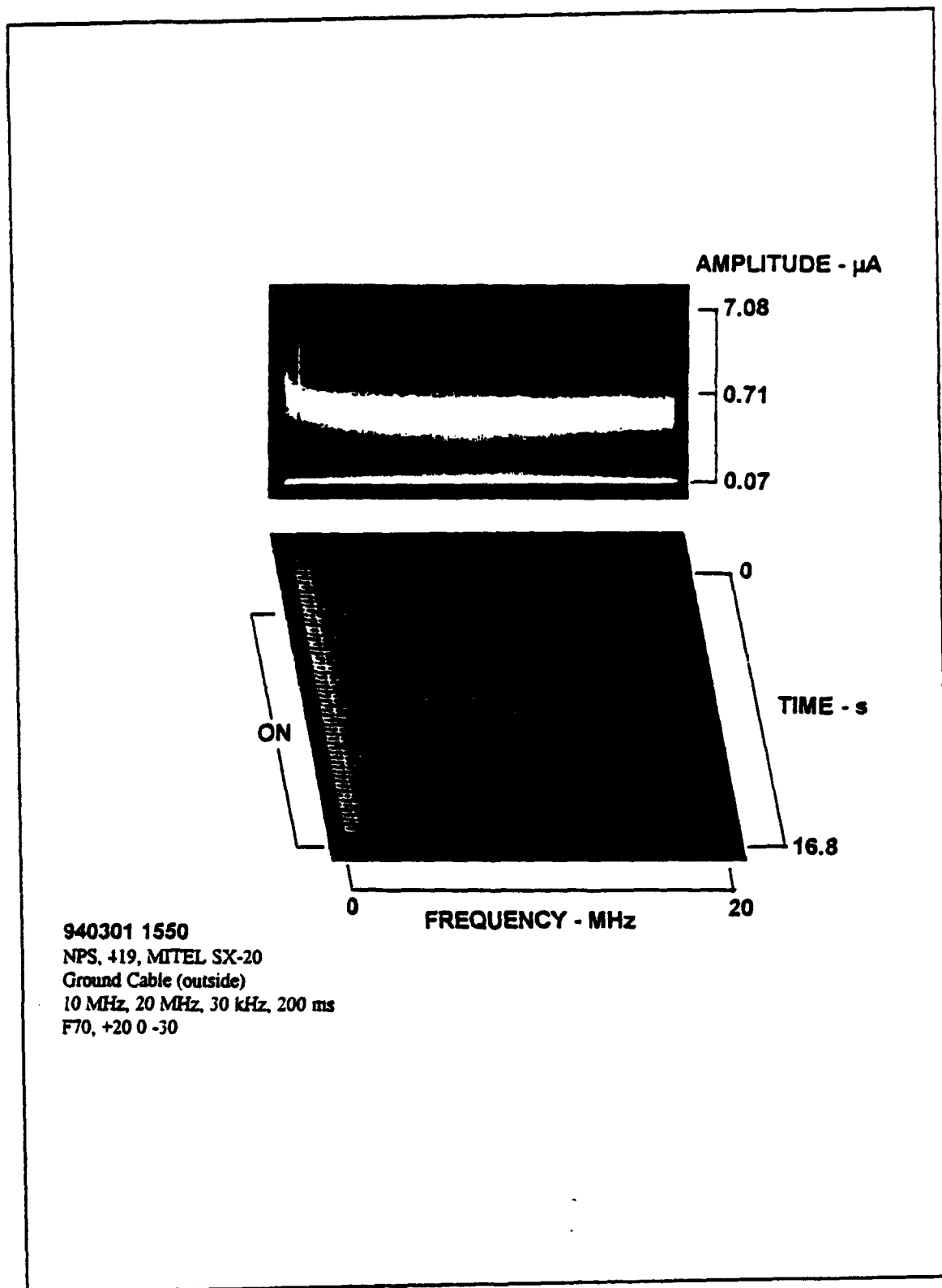


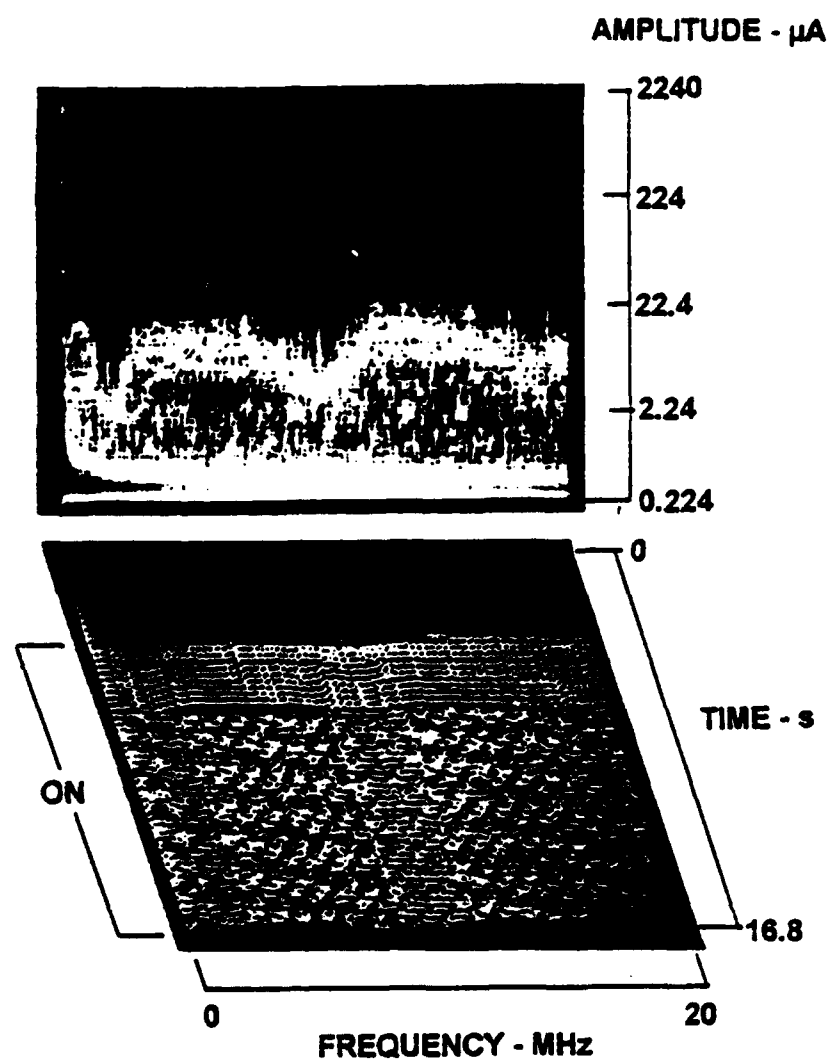
Figure 27. EMI Current on Ground Cable Outside the Cabinet

C. TELEPHONE LINE MEASUREMENTS

As was earlier described, a 30-foot long single-pair telephone wire penetrated the external part of the cabinet through a 1-inch opening at the rear plate. One end of this wire was connected to the telephone wiring block inside the cabinet and the other end was connected to a SUPERSET-3 Telephone Set.

Figure 28 shows EMI current on the telephone wire inside the barrier. The view used an observation time of 16.8 seconds over a frequency range of 0 to 20 MHz. At about 4 seconds, the MITEL SX-20 system was turned on. EMI current appears with an amplitude of about 20 microamperes during the first 4 seconds of operation, and with an amplitude of about 16 microamperes during steady-state operation. At a frequency of about 10 MHz, a null in the current occurred where the amplitude decreased to about 12 microamperes.

Figure 29 shows the EMI current flowing on the telephone wires outside the barrier. An observation time of 16.8 seconds was used over a frequency range of 0 to 20 MHz. At about 4 seconds the MITEL SX-20 system was turned on. Low level EMI current appeared at frequencies of



940225 0916

NPS, 419, MITEL, Telephone Line (inside)

10 MHz, 10 MHz, 30 kHz, 200 ms

F70, +20, 0, -20

Figure 28. EMI Current on Telephone Line Inside the Cabinet

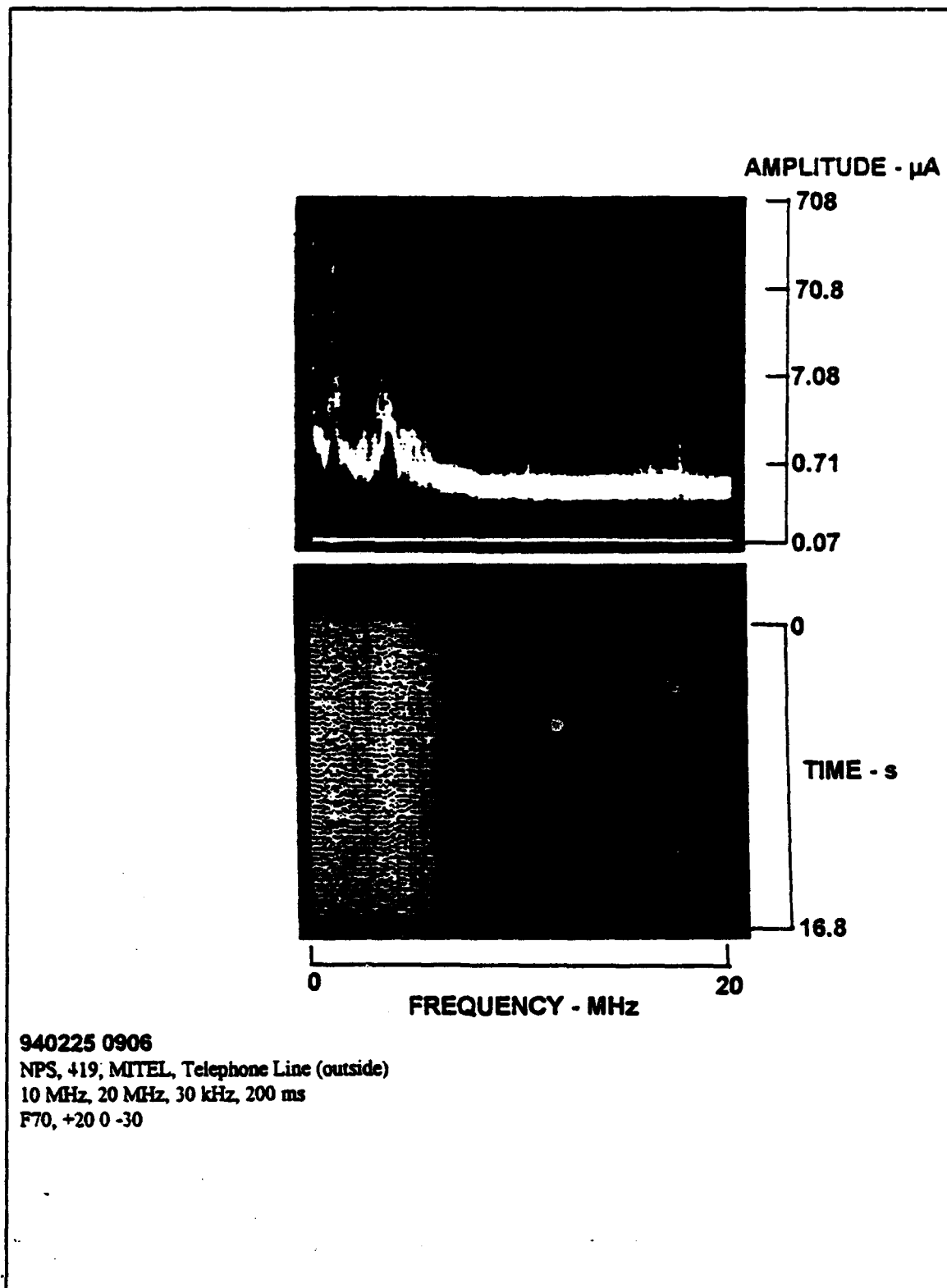


Figure 29. EMI Current on Telephone Line Outside the Cabinet

about 10 and 18 MHz, with amplitudes of about 1.4 and 2.4 microamperes respectively. EMI current over the rest of the band are below the ambient noise, which has an amplitude of about 0.7 microamperes.

In Figure 30 the ambient EMI levels on the telephone line inside and outside the barrier, are shown in a single time-history view. The frequency range was changed to an upper frequency limit of 10 MHz to show ambient EMI current on the external telephone line. The MITEL SX-20 system was turned off during this measurement. The same observation time of 16.8 seconds was used. The outside ambient noise did not enter the barrier. The desirable electromagnetic separation was achieved by the integrated barrier, filter and ground (BFG) configuration.

D. POWER LINE MEASUREMENTS

Two power-line filters were mounted at the rear plate of the cabinet. A two-foot power cable was used inside the barrier to connect the MITEL SX-20 power plug with the one of the filters. A distinct change in the EMI current at the time of turn-on is shown in Figures 31, 32 and 33.

Figure 31 shows the EMI current flowing on the two foot power cable inside the cabinet. An observation time of 16.8 seconds was used over a

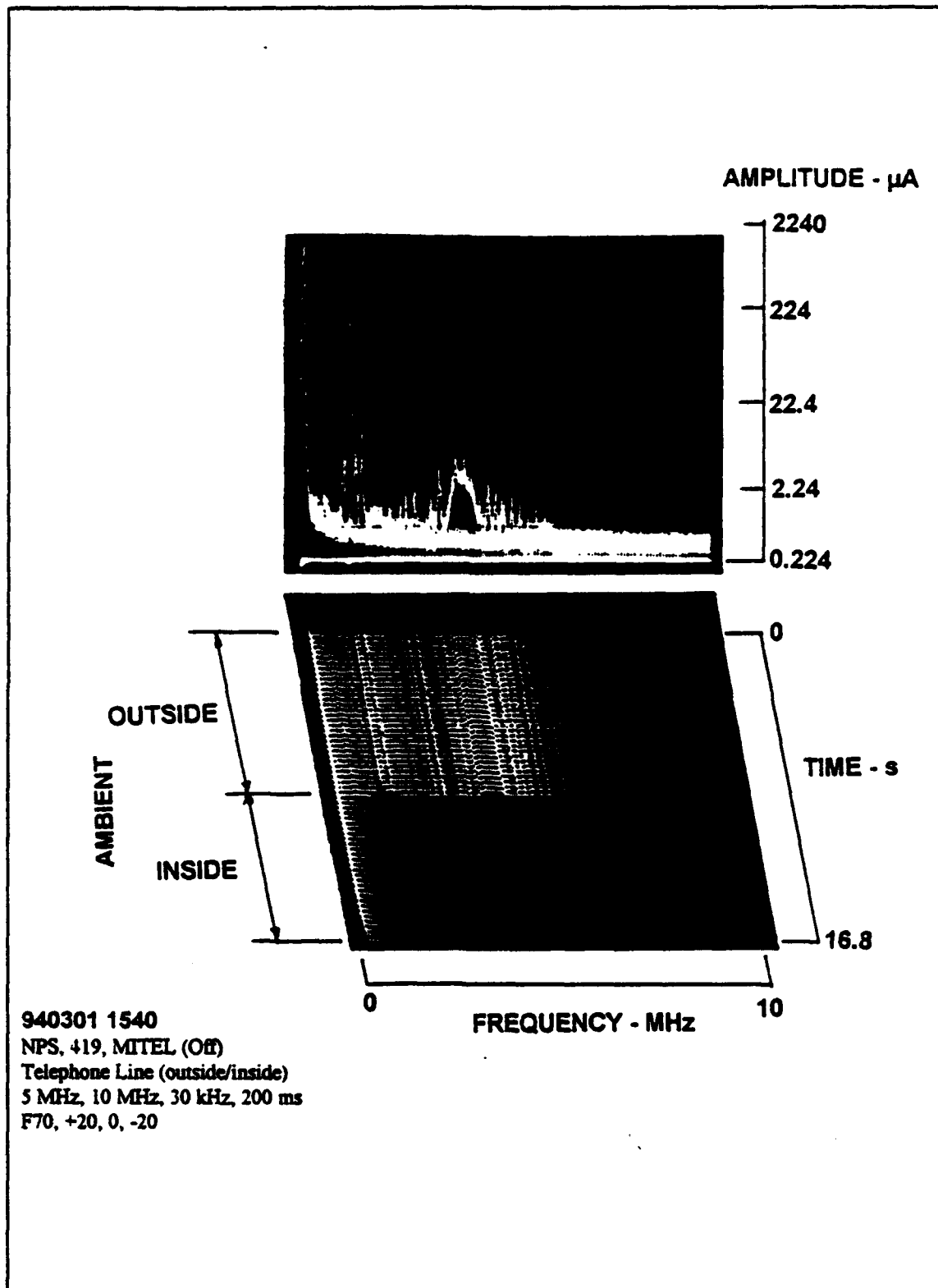
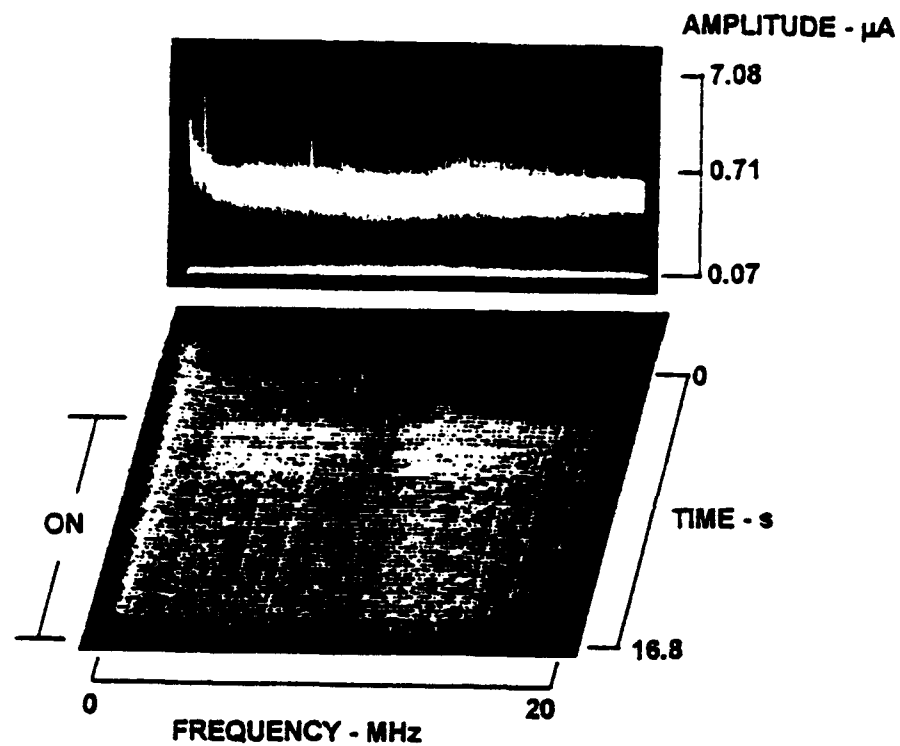


Figure 30. Ambient Noise on Telephone Line Outside/Inside the Cabinet

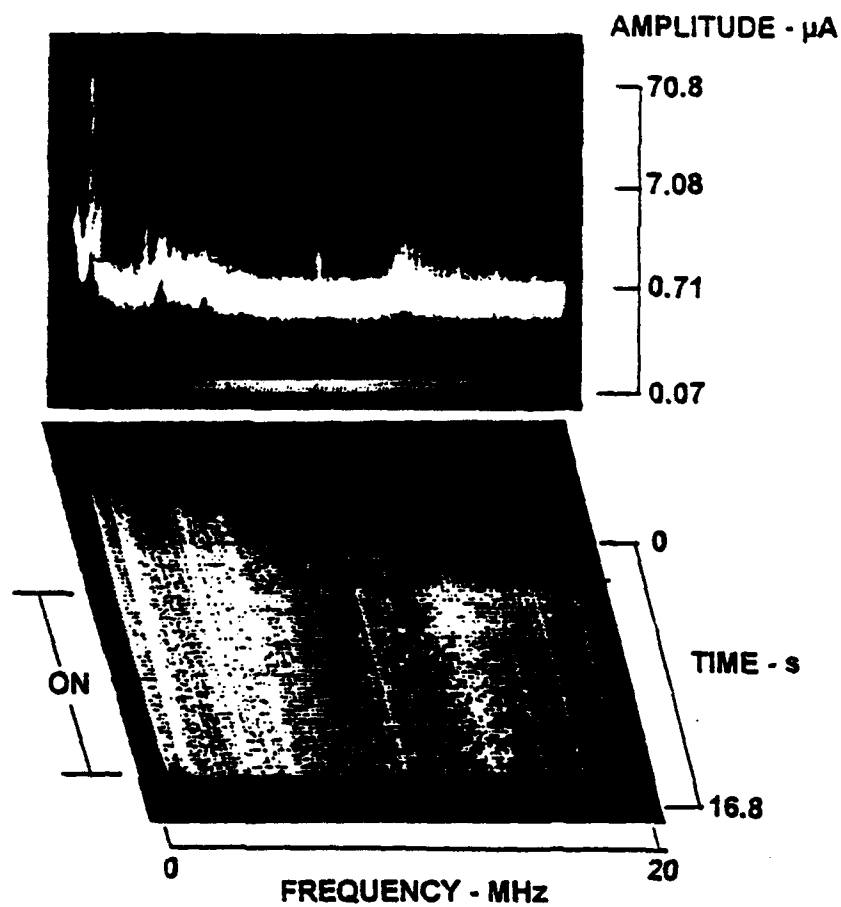


940301 1520
 NPS, +19, MITEL SX-20
 Power Line (inside) with Single Stage Filter
 10 MHz, 20 MHz, 30 kHz, 200 ms
 F70, +20 0 -30

Figure 31. EMI Current on Power-Line Inside the Cabinet (single-stage power-line filter)

frequency range of 0 to 20 MHz. The single-stage power-line filter was used. At about 4 seconds the MITEL SX-20 system was turned on. A very low level of EMI current was found inside the barrier with an amplitude of about 0.8 microamperes. This is not consistent with the EMI current found on the power conductors without the barrier as shown in Figure 25. The barrier cabinet was removed and the EMI current on the power conductors re-examined to determine if the operation of the MITEL SX-20 system had changed for some reason. The EMI current returned to its original spectral and temporal shape. Apparently, the barrier surface provided a partial return path for some of the internal EMI current and reduced the amplitude of the current on the internal power conductor.

Figure 32 shows the EMI current on the power conductors outside the barrier. An observation time of 16.8 seconds over a frequency range of 0 to 20 MHz was used. The single-stage power-line filter was used. At about 4 seconds the MITEL SX-20 system was turned on. As is shown at the top picture in Figure 32, the EMI current is concentrated around frequencies of 4 and 14 MHz with an amplitude of about 4 microamperes. EMI current on the rest of the band is below of 0.8 microamperes and thus, is covered by the ambient noise.



940301 1525
 NPS, 419, MITEL SX-20
 Power Line (outside) with Single Stage Filter
 10 MHz, 20 MHz, 30 kHz, 200 ms
 F70, +20 0 -30

Figure 32. EMI Current on Power-Line Outside the Cabinet (single-stage power-line filter)

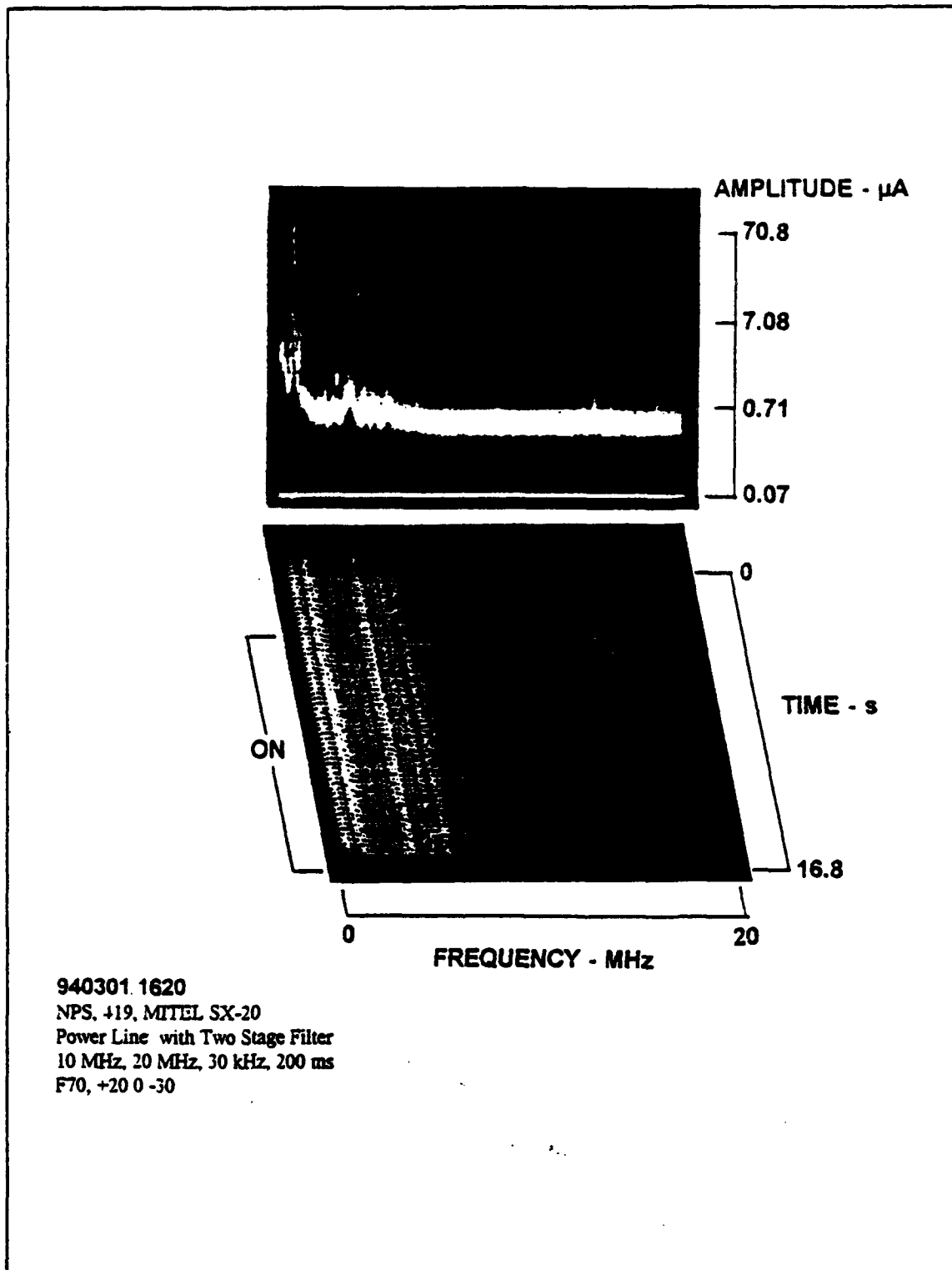


Figure 33. EMI Current on Power-Line Outside the Cabinet (two-stage power-line filter)

In Figure 33 the two-stage power-line filter was used. The observation time was 16.8 seconds over a frequency range of 0 to 20 MHz. At about 4 seconds the MITEL SX-20 system was turned on. No significant EMI current was found. The barrier, filter, and ground (BFG) configuration achieved the goal of reducing EMI current below the ambient noise level.

VII. CONCLUSIONS AND RECOMMENDATIONS

A. CONCLUSIONS

In this study, the temporal and spectral properties of EMI generated by the MITEL SX-20 Automatic Digital Telephone Switching System have been examined over the frequency range of 0 to 100 MHz. EMI currents from the MITEL SX-20 were then sufficiently reduced by the topological method of controlling EMI current.

Following this method, an integrated barrier, filter and ground (BFG) enclosure was constructed and tested for its effectiveness in isolating noise sources from sensitive equipment. The study and measurements provided a number of interesting and useful results. The conclusions drawn are summarized as follows:

- A significant amount of EMI is produced by the MITEL SX-20 system that must be controlled by the integrated BFG configuration. This EMI is conducted or radiated out of the system cabinet over power wires, telephone lines, and ground conductors that penetrate the metallic walls of the equipment cabinets.
- The integrated BFG technique was shown to provide an effective means to control and limit MITEL system generated EMI to harmless levels.

- The isolation that the BFG configuration provides is sufficient over the entire range of 0 to 100 MHz. Therefore, the performance of nearby sensitive radio receivers is not degraded and the reception of Signals of Interest is not affected from EMI generated by the modified MITEL SX-20 system.
- Barrier control is based on the simple concept of controlling the flow of current produced by sources of EMI. For external EMI sources a current return path back to the source is provided without entering the barrier. For EMI sources within the cabinet, a return current path back to the source is provided without leaving the cabinet.
- The successful implementation of barrier control at the cabinet level, mainly depends on the proper control of all penetrating conductors that can conduct or radiate EMI into or out of a cabinet.
- The grounding of the cabinet has special importance in this technique. In the BFG configuration for MITEL SX-20 system, the external cabinet ground conductors did not directly penetrate the wall of the cabinet. The external ground was attached to the external surface of the barrier. The internal ground conductor was attached to the internal surface of the barrier. The internal green wire of the power conductor was also attached to the inside of the barrier.
- All sensitive signal conductors must be double-shielded and standard coaxial bulkhead connectors must be used at the cabinet walls for all penetrating conductors.
- In the BFG technique, power-line filters must be installed at a barrier wall. These filters must provide a path for the flow of internally and externally generated EMI current back to its source.

B. RECOMMENDATIONS

After having examined the temporal and spectral properties of EMI generated by the MITEL SX-20 system and its elimination by using the topological approach method, the following recommendations can be made:

- Design and produce all new equipment and all modified equipment, in accordance with barrier control principles.
- Repeat the same experiment for other digital systems such as personal computers, laser printers etc. that generate EMI.
- Use the topological approach method for the control of EMI for other applications such as cabinets, shielded rooms, and entire buildings.

LIST OF REFERENCES

1. Adler, R.W., Notes for EC 3640 (Electromagnetic Environmental Effects), Naval Postgraduate School, 1993 (unpublished).
2. Ficchi, R.F., *Practical Design for Electromagnetic Compatibility*, pp. 1-31, Hayden Book Company, Inc., New York, 1971.
3. Grodek, T.L., *Practical Considerations of the Topological Approach to Electromagnetic Interference Control*, Master's Thesis, Naval Postgraduate School, Monterey, California, March 1986.
4. Ingram, V.D., *Strategies in the Topological Approach to Electromagnetic Interference Control*, Master's Thesis, Naval Postgraduate School, Monterey, California, December 1987.
5. *Performance Evaluation at Cryptologic Sites Technical Course Manual*, Draft 1, Chapters 4 and 7, Signal-to-Noise Enhancement Program (SNEP) Team, April 1991.
6. Vincent, W.R. and Munsch, G.F., *Power Line Noise Mitigation Handbook*, 2nd ed., Southwest Research Institute, San Antonio, Texas, January 1993.
7. Skomal, E.N., *Man-Made Radio Noise*, Van Nostrand Reinhold Co., New York, 1978.
8. Ott, H.W., *Noise Reduction Techniques in Electronic Systems*, John Wiley and Sons, 1976.
9. Freeman, E.R., *Electromagnetic Compatibility Design Guide*, (NAVAIR AD 1115), Artech House, Dedham, MA., 1982.
10. Paul, C.R., *Introduction to Electromagnetic Compatibility*, John Wiley and Sons, Inc., 1992.

11. Horowitz, P. and Hill, W., *The Art of Electronics*, 2nd ed., Cambridge University Press, 1989.
12. Graf, W. and Vance, E.F., "*Elements of a Topological Barrier for Electromagnetic Interference Control*," IEEE International Symposium on Electromagnetic Compatibility, Santa Clara, CA., pp.46-48, 1982.
13. Cooper, G.R. and McGillem, C.D., *Probabilistic Methods of Signal and System Analysis*, 2nd ed., Holt, Rinehart and Winston, Inc., 1986.
14. Mikros, E., *Mitigation of EMI/RFI produced by a 1.2 kW Uninterruptible Power Supply*, Master's Thesis, Naval Postgraduate School, Monterey, California, September 1993.
15. *SX-20 Superswitch*, Mitel Standand Practice Generic 503, Mitel, March 1985

INITIAL DISTRIBUTION LIST

	No. Copies
1. Defense Technical Information Center Cameron Station Alexandria VA 22304-6145	2
2. Library, Code 52 Naval Postgraduate School Monterey, CA 93943-5101	2
3. Chairman, Code EC Department of Electrical and Computer Engineering Naval Postgraduate School Monterey, CA 93943-5121	1
4. Professor Richard W. Adler, Code EC/Ab Department of Electrical and Computer Engineering Naval Postgraduate School Monterey, CA 93943-5121	5
5. Professor Wilbur R. Vincent, Code EC/Ab Department of Electrical and Computer Engineering Naval Postgraduate School Monterey, CA 93943-5121	3
6. Chris Adams ManTech 6593 Commerce Ct. Gainsville, VA 22065	1

- | | | |
|-----|-------------------------------------------------------------------------------------------------------|---|
| 7. | Roy Bergeron
ERA
1595 Spring Hill Rd.
Vienna, VA 22180 | 1 |
| 8. | Anne M.G. Bilgihan
USA INSCOM MSA-V EAQ
Bldg 160 MS Vint Hill Farms
Warrenton, VA 22186-5160 | 1 |
| 9. | Roy Dossat
SPAWARS Code PMW 144-3
NC1 3E52, Arlington, VA 20363 | 1 |
| 10. | Jim Engels
NESSEC Code 0411
3801 Nebraska Ave. NW
Washington, DC 20393 | 1 |
| 11. | Pamela Guardabascio
NESSEC Code 0411
3801 Nebraska Ave. NW
Washington, DC 20393 | 1 |
| 12. | George Hagn
SRI International
1611 N. Kent St.
Arlington, VA 22209 | 1 |
| 13. | Leo Jonas
USAF ESC/LEMP
San Antonio, TX 78243-5000 | 1 |
| 14. | Sherry M. Jordan
US ARMY INSCOM/MSA-V Bldg160
Vint Hills Farms
Warrenton, VA 22186 | 1 |

- | | |
|-----------------------------------------------------------------------------------------------------------------|---|
| 15. Steve Kelly
NESSEC Code 0411A
3801 Nebraska Ave. NW
Washington, DC 20393-5210 | 1 |
| 16. Brian I. Kutara
NEEACT PAC
Box 130
Pearl Harbor, HI 96860-5170 | 1 |
| 17. CDR Gus Lott
Naval Security Group Command, Code GX
3801 Nebraska Ave. NW
Washington, DC 20393-5210 | 1 |
| 18. George F. Munch
160-CR-375
San Antonio, TX 78253 | 1 |
| 19. Hugh Myers
NEEACT PAC
Box 130
Pearl Harbor, HI 96860-5170 | 1 |
| 20. LCDR Andrew Parker
US Naval Academy
Dept. of Electrical Engr.
Annapolis, MD 21402 | 1 |
| 21. Jane Perry
1921 Hopefield Rd.
Silver Spring, MD 20904 | 1 |
| 22. Art Reid
1177 Bollinger Rd.
Littlestown, PA 17340 | 1 |

- | | | |
|-----|------------------------------------------------------------------------------------------|---|
| 23. | Miquel I. Sanchez
NSA Code G042
Fort Meade, MD 20755-6000 | 1 |
| 24. | Embassy of Greece
Naval Attache
2228 Massachusetts AVE., NW
Washington, DC 2008 | 1 |
| 25. | Emmanuel Stelioudakis
92 Tritonos St.
Palaio Faliro 17562
Athens
Greece | 1 |